Kirkuk Journal of Science Vol. 21, Iss. 2, p. 1-23, 2026 doi:10.32894/kujss.2026.168996.1283

Synthesis, Characterization, and Antibacterial Activity of Binuclear Metal Complexes with Macrocyclic Schiff Base Ligand and DFT Studies.

Marjan M. Islam *, Salwan I. Mohammed

Department of Chemistry, College of Science, University of Duhok, Duhok, Iraq.
*Corresponding author : marjan.islam@uod.ac.

Article Information

Article Type:
Research Article

Keywords:
macrocyclic Schiff base ligand; N4 donor; Antibacterial activity; DFT; Binuclear.

History:
Received: 26 January 2026
Revised: 24 April 2026
Accepted: 24 April 2026
Available Online: 30 June 2026

Citation: Marjan M. Islam, Salwan I. Mohammed, Synthesis, Characterization, and Antibacterial Activity of Binuclear Metal Complexes with Macrocyclic Schiff Base Ligand and DFT Studies., Kirkuk Journal of Science, 21(2), p. 1-23, 2026, https://doi.org/10.32894/kujss.2026.168996.1283

Abstract

A new Series of binuclear macrocyclic Schiff base complexes with the general formula $[M_2LCl_4]$, (M = Mn (II), Fe(II), Co(II), Ni(II), Cu(II), Zn(II)) was synthesized and characterized, the macrocyclic ligand L = (2Z, 21Z) -3, 10, 14, 21-tetraaza-1, 12(1, 4)- dibenzenacyclodocosaphane-2, 10, 13, 21-tetraene) was obtained through a 2:2 condensation reaction of Terephthalaldehyde with Hexamethylenediamine, forming a stable N_4 macrocycle. The synthesized compounds are characterized by FT-IR, UV–Vis, atomic absorption spectroscopy (AAS), molar conductivity, magnetic susceptibility measurements, and ^{1}H and ^{13}C NMR spectroscopy. The combined spectroscopic, analytical, and magnetic data are consistent with a tetrahedral environment around the metal centers in all complexes except the Cu(II) complex, which exhibits a square planar geometry. The complexes exhibit non-electrolytic behavior in solution, as inferred from molar conductivity measurements. The disc diffusion method was used to evaluate the antibacterial activity of the Schiff base ligand and its metal complexes. The result demonstrated that metal coordination significantly enhances the ligand's capacity to inhibit the growth of both Gram-positive and Gram-negative bacteria (Staphylococcus aureus, Escherichia coli, and Klebsiella pneumoniae). Density functional theory (DFT) calculations were performed at the B3LYP level using the LANL2DZ basis set for the metal atoms and 6-311++G(d,p) for the non-metal atoms. The calculations provided optimized geometries, HOMO–LUMO energies, and thermodynamic parameters, which supported the experimental results and offered further insight into the metal–ligand interactions governing the stability and reactivity of the complexes.

1. Introduction:

Schiff bases constitute a broad class of organic compounds characterized by the presence of an imine (-C=N-) functional group [1], [2], [3]. They are typically formed through the condensation reaction between aliphatic or aromatic amines with aldehydes or ketones containing a reactive carbonyl group [4]. The formation of Schiff bases generally proceeds via nucleophilic attack of the amine on the carbonyl carbon, followed by elimination of water. Depending on the electronic properties of the substrate, this process can be accelerated by either an acid or base catalyst, or by the application of elevated temperature [5], [6].

The broad applicability of Schiff bases is primarily attributed to the strong donor ability of the azomethine nitrogen atom, which acts as an effective electron donor and enables Schiff bases to coordinate readily with metal ions, thereby attracting considerable scientific interest in both ligand design

and metal-complex synthesis [7]. Schiff bases are substantial due to their stability, chelating properties, and biological applications [8]. The rise of antibiotic-resistant organisms has increased the importance of identifying new antibacterial medicines with improved selectivity and reduced toxicity [9]. Schiff bases and their metal complex have also been shown to have antibacterial, antifungal, and anticancer properties [10]. They are effective antibacterial agents, Metal complexation can significantly improve biological activity and alter microbial susceptibility [11], [12]. Schiff-base macrocyclic ligands and their metal complexes represent an essential class of compounds that have been extensively investigated. Macrocyclic tetradentate Schiff base ligands are significant in coordination chemistry due to their four donor sites, which provide robust and versatile binding [13], as shown in Figure 1.

The synthesis of tetraazamacrocyclic complexes has been significantly aided by condensation reactions between diketones and primary diamines in the presence of metal ions.The metal facilitates the process by directing the steric course toward cyclic molecules rather than polymeric structures. Macrocyclic complexes exhibit greater thermodynamic stability and enhanced selectivity as ion binders compared to their open-chain analogs [14], [15]. Their cyclic framework generates stable metal complexes with various structural features, making them significant in catalysis, bioinorganic chemistry, and medical applications [16]. Macrocyclic Schiff ligands, particularly when coordinated with transition metals, have attracted significant attention because of their structural diversity and their ability to influence the physicochemical and biological properties of the resulting metal complexes [17].

In the present study, a novel Schiff base ligand and its symmetrical binuclear azomethine complexes of Mn(II), Fe(II), Co(II), Ni(II), Cu(II), and Zn(II) were successfully synthesized and characterized, These complexes were prepared through the condensation of Terephthalaldehyde and 1, 6-hexamethyle-nediamine (Figure 2). The tetradentate Schiff base ligand and all the six complexes were identified and characterized using NMR, IR, UV-Visible spectroscopy, atomic absorption, molar conductivity, and magnetic moment measurement. They were examined for their antibacterial efficacy against Escherichia coli, Staphylococcus aureus, and Klebsiella Pneumonia to assess the influence of metal-ion identity and macrocyclic coordination on biological effectiveness.

Furthermore, Density Functional Theory (DFT) calculations were carried out using the B3LYP functional. The 6-311++G(d,p) basis set was used for non-metal atoms (C, H, and N), while the LANL2DZ basis set was employed for the transition metal ions. Gaussian 16 software was used for geometry optimization and the calculation of structural parameters, including bond lengths and bond angles. The frontier molecular orbitals (FMOs),(HOMOs and LUMOs)were also investigated. The global reactivity descriptors were derived from FMO energy-level analysis. Providing optimized geometries, HOMO–LUMO energy gaps, and electrostatic potential assessments of the molecules. The thermodynamic parameters were calculated in both the gas and solvent phases to evaluate the effect of solvation on the stability of the studied compounds.

2. Materials and Methods:

All solvents and reagents used in this work were of analytical quality. Most chemicals were supplied by the University of Duhok, including $MnCl_2{\cdot}4H_2O$, $FeCl_2{\cdot}\ 4H_2O$, $CoCl_2{\cdot}\ 6H_2O$, $NiCl_2{\cdot}\ 6H_2O$, $CuCl_2{\cdot}\ 2H_2O$, $ZnCl_2$, hexamethylenediamine, ethanol, and diethyl ether. Additionally, Terephthalaldehyde was purchased from Bide Pharmatech Ltd, glacial acetic acid from Scharlau, and DMF from Thomas Baker. The ^{1}H and ^{13}C-NMR spectra of the synthesized ligand were recorded on a Bruker Ultra Shield 500 MHz NMR spectrometer in $CDCl_3$ at 298 K. FTIR spectra were obtained using a Shimadzu FTIR-8400S spectrophotometer in the 4000–400 cm^{-1} range with KBr discs.

Magnetic susceptibility measurements were performed in the solid state at 298 K using a Sherwood Scientific magnetic balance. Electronic absorption spectra were recorded at 25 ^{o}C in DMF using a Jenway 6800 double beam UV–Vis spectrophotometer 10^{-3} M with 1 cm quartz cells. The melting and decomposition temperatures of the ligand and its complexes were determined using an electrothermal melting point apparatus. Molar conductivity measurements were carried out using a 4520PH conductivity meter for 10^{-3} M DMF solutions at 25^{o}C. Metal ion contents of the complexes were finally quantified using an AA-670G Atomic absorption spectrophotometer. The disc diffusion method was used to measure antibacterial activity. The geometries and energies of these compounds were assessed using Gaussian 16W.

2.1 Synthesis of Schiff Base Ligand [$C_{28}H_{3}6N_4$]:

The synthetic route of the macrocyclic Schiff base ligand by mixing (0.02mol, 2.6822g) Benzene-1, 4-dicarboxaldehyde in 70ml of ethanol with (0.02 mol, 2.323g) hexamethylenediamine in 50ml of ethanol, under continuous magnetic stirring. Subsequently, three droplets of glacial acetic acid were added as a catalyst. The reaction mixture was refluxed for 8 hours at 80 ^{o}C. The precipitate formed was then filtered, thoroughly washed with ethanol and diethyl ether, and dried in vacuo over anhydrous $CaCl_2$. A pale-yellow solid was obtained, yielding 4.0751 g (95.09%) and a melting point of 176 ^{o}C. H-NMR, 500 MHz; $CDCl_3$) δ 8.27 (s,1H), 7.747 (s, 2H), 3.62 (t, 2H), 1.77 – 1.35 (m, 4H). ^{13}C-NMR (125 MHz, $CDCl_3$) δ 160.28, 138.07, 128.23, 77.03, 76.77, 61.83, 30.81, 27.17.

2.2 Synthesis of Binuclear Metal (II) Complexes:

2.2.1 Synthesis of [Ni_2($C_{28}H_{36}N_4$) Cl_4] Complex:

The complex was prepared by reacting (0.001 mol,0.428 g) of the ligand in 15 mL of Chloroform, which was then

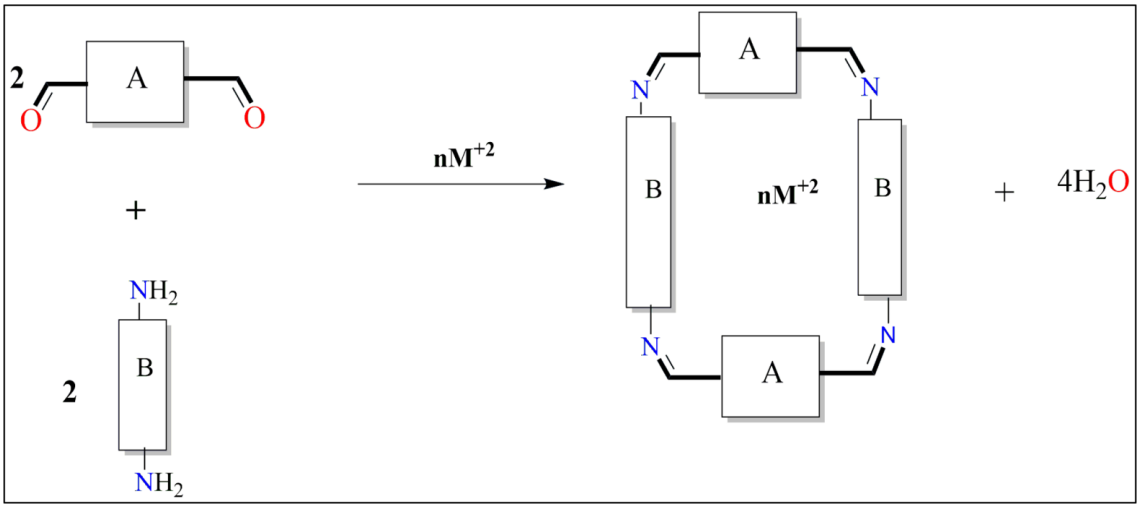

Figure 1. The macrocyclic formation reaction, where A and B represent aliphatic or aromatic (dialdehyde and diamine), n is the number of moles of M(II) transition metals.

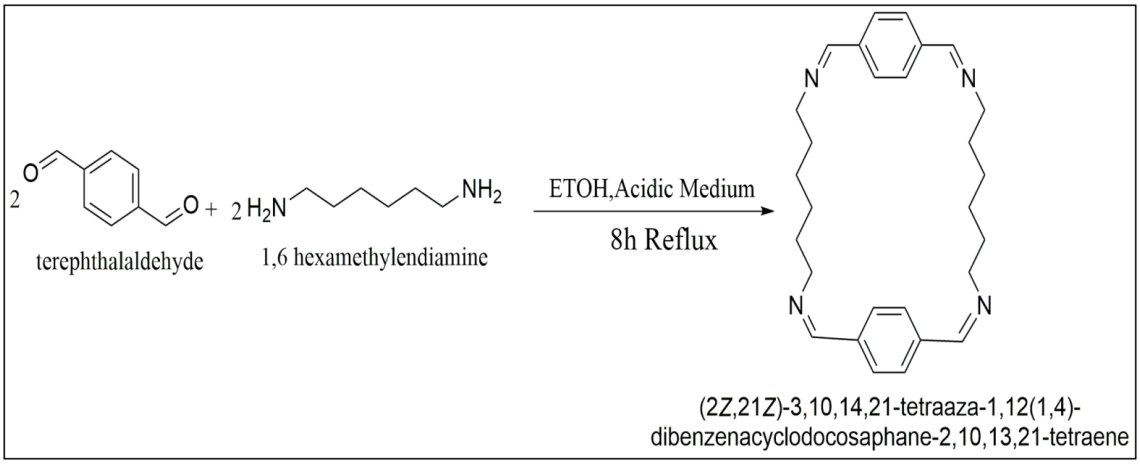

Figure 2. Synthesis of Schiff Base Ligand.

placed in an ultrasonic bath for approximately 20 minutes. An ethanolic solution of $NiCl_2 \cdot 6H_2O$ (0.002mol, 0.4753 g) was added dropwise to the ligand solution. The mixture was refluxed for approximately 9 hours at 80^{o}C. The olive- green resultant solid complex was filtered, thoroughly washed with ethanol and diethyl ether successively, and subsequently dried at room temperature. Yield (0.6076 g), (88.35%), m.p (224) Dec.

2.2.2 Synthesis of the additional metal ions complexes $[M_2(C_{28}H_{36}N_4)\ Cl_4]$:

A series of transition metal complexes with the general formula $[M_2LCl_4]$, M = Mn(II), Fe(II), Co(II), Ni(II), Cu(II), Zn(II),were synthesized following the same procedure described for the nickel complex. The corresponding metal salts were used in 0.002 mol quantities: M=$MnCl_2$.4H2O (0.3985g), $FeCl_2$.4H2O (0.3976g), $CoCl_2$.6H2O (0.475g), $CuCl_2.2H_2O$ (0.340g), $ZnCl_2$ (0.2725g). Each metal salt solution was added dropwise to a chloroform solution of the ligand (0.001mol) that had been previously subjected to ultrasonication, followed by reflux. The solids were filtered, washed with Ethanol and diethyl ether, dried at room temperature. All complexes were subsequently subjected to physicochemical and some spectroscopic characterization. The synthetic route adopted for the preparation of the binuclear Schiff base complexes is illustrated in Figure 3."

2.3 Computational Aspects:

In chemistry and physics, density functional theory (DFT) is a valuable technique for determining the electronic structure of atoms, molecules and solids [18]. Electronic structure calculations play a crucial role in elucidating chemical structure and reactivity [19]. By advancing the development of computational chemistry, density functional theory (DFT) has been widely employed owing to its accuracy and low computational cost in calculating a broad spectrum of molecular properties, yielding reliable results that align with experimental data [20].

The geometries of the free ligand and its transition-metal complexes were optimized using the Gaussian 16 program. Geometry optimization calculations were carried out within the framework of density functional theory (DFT) employing the B3LYP functional. The 6-311++G (d,p) basis set was applied to the ligand atoms (C, H, and N), whereas the LANL2DZ basis set was used for the metal centers (Mn, Fe, Co, Ni, Cu, and Zn). This computational level was selected because it has been widely employed in studies of organic, coordination, and organometallic systems, offering a practical balance between computational cost and accuracy in describing ground-state geometries and electronic structures [21], [22]. We employed the computational protocol to determine the optimal bond lengths, bond angles, thermodynamic parameters and frontier molecular orbital energies (FMOs). Examining the energy of the (HOMO and LUMO)is especially crucial as variation in their energy separation illustrates how metal coordination influences the reactivity and stability of the complex [23], [24]. This is particularly relevant when considering the HOMO–LUMO energy gap associated with these orbitals. To identify the electrophilic and nucleophilic regions, the molecular electrostatic potential is employed [25].

2.4 Antibacterial Efficacy:

Antibacterial activity was assessed using clinical isolates collected from Sheryan Hospital. The antibacterial activity of the free ligand and its complex was evaluated against Staphylococcus aureus (a Gram-positive bacterium), Klebsiella pneumoniae, and Escherichia coli (two Gram-negative bacteria). Antibacterial activity was evaluated using the disc diffusion method according to the Clinical and Laboratory Standards Institute (CLSI) guidelines [26].

Each bacterial strain was cultured into 5 mL of Brain Heart Infusion Broth using a single well-isolated colony. The cultures were subsequently incubated at 37 ^{o}C for 18–24 h. To cover the surface of the Muller-Hinton agar (MHA) plates with bacteria in three different orientations we used a sterile cotton swab that had been submerged in the bacterial suspension. The plate was rotated 60 degrees between streaks, and the edges were cleaned thoroughly to ensure the germs were spread evenly. The ligand and its complexes were dissolved in DMF (10^{-3} M), and 5 mm filter paper discs were dipped into the solutions, which were then allowed to dry in a sterile environment. Discs were aseptically arranged on inoculated agar plates at distances of 30–36 mm to prevent overlapping inhibition zones. Every single dish maintained a precise temperature of 37 ^{o}C for more than 24 hours in an incubator. The circumference of the inhibition zone encircling the disc was measured after the incubation period [27].

3. Results and Discussion:

Experimental and theoretical results on the synthesis of a macrocyclic Schiff base ligand and its transition metal complex are presented. Synthesis of the coordination complexes is confirmed by spectroscopic, physicochemical, and theoretical investigations. The ligand was synthesized via a conventional condensation reaction between Hexamethylenediamine or 1,6-Hexanediamine and Terephthalaldehyde in a 2:2 molar ratio under acid-catalyz-ed conditions. They further reveal the role of metal ions in modifying ligand structure and electrical properties. The combination of the applied characterization techniques provides insight into metal–ligand interactions and the geometries adopted by the complexes.

Computational results support experimental data, with optimized geometries and HOMO-LUMO distributions illustrating the electronic structure. Furthermore, calculated reactivity descriptors provide a quantitative basis for the observed chemical stability. The calculated energies and thermodynamic parameters were interpreted in a comparative manner within the same computational framework to evaluate relative

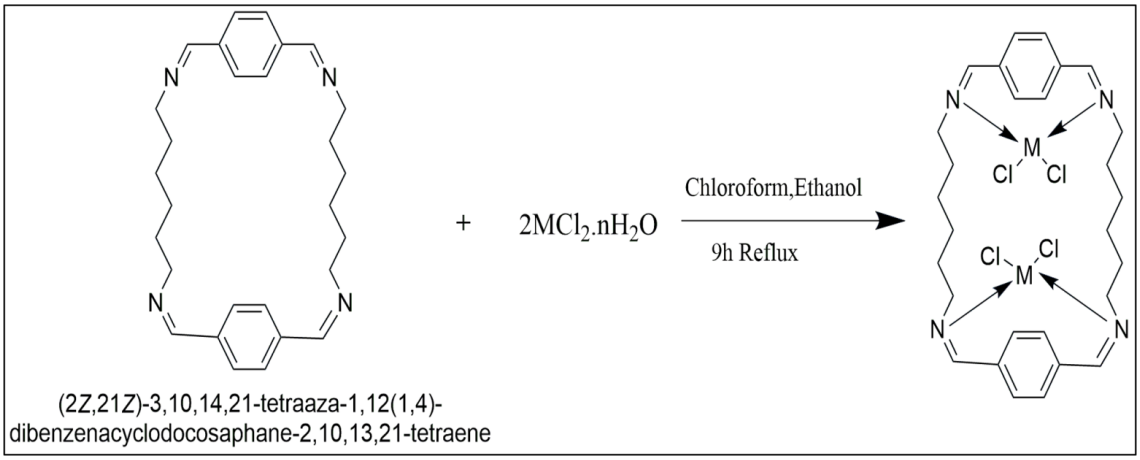

Figure 3. Synthesis of Schiff Base Complexes, where M=Mn(II), Fe(II), Co(II), Ni(II), Cu(II), Zn(II), n= 0,2,4,6.

trends among the studied compounds. We measured the molar conductivity of the metal complexes in dimethylformamide (DMF) with values ranging from 19.45 to 34.30 $\Omega^{-1}.cm^2.mol^{-1}$. These low conductivity values indicate that all the compounds behave as non-electrolytes in solution [28]. Table 1 presents key physicochemical data, including melting points, molecular weight, metal percentages, and other critical properties.

3.1 FTIR Analysis:

Infrared spectra in the range 4000-400 cm^{-1} have been obtained for the ligand and its complexes, with the measured frequencies assigned to distinct group vibrations by comparison with spectra of analogous complexes. The characteristic infrared frequencies of the Schiff base and its associated compounds are detailed in Table 2. The magnitude of displacement depends on the interatomic binding energy. Although a medium-to-broad band appears at 3425 cm^{-1}, the absence of the bending vibration (H-O-H) at around 1600-1630 cm^{-1} confirms that no molecular or coordinated water is present. Therefore, the observed band is attributed to moisture introduced by the instrument environment rather than to hydration of the Schiff base.

The aromatic stretching band C-H weak peak was found at 3032-3066 cm^{-1} [29]. Vibrational frequency ranging (2920-2849) cm^{-1} respectively, were for the symmetric and asymmetric stretching vibrational spectra for(C-H)aliphatic [30]. The Ligands IR spectra exhibited no signals around 3300-3200 cm^{-1} for the $\nu(NH_2)$ amino group or around 1716cm^{-1} for the C=O group [31]. This indicated that the NH_2 group had fully reacted with the C=O group, thereby inducing the formation of a macrocyclic structure [32]. Within this spectrum, the Ligand displayed an azomethine stretching frequency at 1639 cm^{-1}, indicating the production of a Schiff base [33], [34]. The infrared spectra of the complexes exhibited ligand bands with associated shifts indicative of complex formation.

The imine stretching band observed in the free Schiff base shifts to a lower frequency, appearing in the range 1587-1608 cm^{-1} in the complexes, signifying the involvement of the azomethine nitrogen atom in coordination with the metal ions [35]. Aromatic C=C stretching vibrations are commonly observed between 1504 and 1579 cm^{-1} in Schiff bases and their metal complexes [36]. The CH2 bending shows between (1456-1498)cm^{-1} [34]. At lower frequencies, the complexes displayed new bands at 418-466 in their vibrational spectra, which were attributed to ν(M-N) frequencies respectively [26], [37]. The coordinated chloride ions cannot be detected as they fall outside the instrument's scale. The silver nitrate test indicates the absence of uncoordinated Cl- ions, as supported by the conductivity measurement [38]. The gas-phase infrared spectra of the synthesized compounds, calculated at the B3LYP/6-311++G(d,p) and LANL2-DZ basis sets, are presented in Table 2. The significant similarity between the real and computed spectra suggests that the molecular structures of the ligand and its corresponding metal complexes are largely equivalent in both the solid and gas phases. The obtained results align well with previous research investigations [39], [40].

3.2 NMR Study of the Schiff Base Ligand:

The chemical structures of the synthesized Schiff Base ligand were elucidated using ^1H and ^{13}C NMR spectroscopy (500 MHz) in $CDCl_3$. The ^1H-NMR spectrum demonstrates successful condensation and structural characterization of the synthesized Schiff base ligand. In azomethine systems generated from aromatic aldehydes and amines, the absence of an aldehydic proton signal (typically near 9-10.0 ppm in the starting materials) is a primary diagnostic of complete imine production, a pattern that has been reported in several Schiff base studies [41]. The presence of a -CH=N proton signal at δ 8.27 ppm(s,1H) [42]. The signal at δ 7.74 ppm corresponds to the aromatic hydrogens [43].

A triplet signal observed at 3.60-3.63 ppm is attributed

Table 1. The physicochemical properties of free ligand and its synthesized complexes.

Compounds	M.wt	Color	m.p (^{o}C)	Molar conductivity $\Omega^{-1}.cm^2.mol^{-1}$	M % Cal Found	Yield %
Ligand	428.6	Pale yellow	176	– – –	– – –	85.09
$[Mn_2LCl_4]$	680	Yellow	279 *	30.4	16.15 15.66	70.56
$[Fe_2LCl_4]$	682.1	Light brown	253 *	22.1	16.37 15.97	65.01
$[Co_2LCl_4]$	688.3	Light green	292 *	30.0	17.12 17.06	66.59
$[Ni_2LCl_4]$	687.8	Olive green	224 *	29.4	17.07 16.90	73.95
$[Cu_2LCl_4]$	697.5	Green	285*	19.45	18.22 17.8	69.73
$[Zn_2LCl_4]$	701.2	Light Orange	207 *	34.3	18.65 18.32	81.93

* =Decomposition, M% = metal percent, Cal = Calculated, M.wt = Molecular weight.

Table 2. The experimental and calculated FT-IR spectra of the SB ligand and its compounds.

Comp	ν(C=N) Exp Cal	ν_{ar} (C=C) Exp Cal	ν_{ar} (C–H) Exp Cal	ν_{ali} (C–H) Exp Cal	δ C–H Exp Cal	M-N Exp Cal
L	1639 1650	1566 1588	3032 3067	2849,2920 2976	1456 1497	–
$[Mn_2LCl_4]$	1581 1596	1579 1582	3045 3056	2856,2929 3031	1488 1512	422 434
$[Fe_2LCl_4]$	1602 1606	1560 1573	3066 3078	2854,2933 3017	1475 1491	449 451
$[Co_2LCl_4]$	1608 1622	1564 1540	3014 3045	2860,2931 3014	1498 1512	418 425
$[Ni_2LCl_4]$	1606 1628	1564 1580	3008 3036	2856,2927 2996	1475 1508	466 461
$[Cu_2LCl_4]$	1604 1622	1573 1559	3040 3084	2854,2927 2997	1465 1488	422 428
$[Zn_2LCl_4]$	1600 1624	1569 1540	3060 3084	2858,2923 2995	1461 1488	424 428

ν = Stretching , δ = bending.

to the methylene protons adjacent to the imine nitrogen CH= N-CH2 [34]. The signal from 1.35-1.77ppm in the ^{1}H-NMR spectrum of the Schiff base ligand results from protons of the methylene -CH2- group [44]. The ^{13}C NMR spectra of the Schiff base ligands were obtained using $CDCl_3$ as the solvent. In the spectra, the signal area at 160.28 ppm confirms the formation of azomethine [45].The chemical shifts of the aromatic carbon in this Ligand were determined to be 128.23, 138.07ppm [5]. Strong signals from (76.77,77,03) δ belong to the $CDCl_3$ Solvent [46]. The CH2-N=C contributed to the signal observed at 61.83ppm in the Schiff Base Ligand [47]. The 13C NMR spectrum of this molecule demonstrated peaks at δ 27.17 and 30.81 ppm ascribed to the methylene carbons CH2-CH2-[34], as shown in Figures 4 and 5.

3.3 Electronic spectra – magnetic moment:

The electronic spectra of the Schiff base ligand and its metal complexes were recorded in DMF solution, 0.001 M. The results are summarized in Table 3. The corresponding UV–Visible spectra of the ligand and its metal complexes are presented in Figure 6. The UV-Vis spectrum of the free Schiff base ligand exhibited absorption peaks within the range of(47846-35587)cm^{-1}, (34246-29239)cm^{-1}, which can be attributed to $\pi \rightarrow \pi*$ and n $\rightarrow \pi*$ transitions associated with the azomethine group and aromatic ring of the ligand [48], [49], [50]. The Mn(II) complex displays a magnetic moment of 5.7 B.M, which correlates closely with the calculated spin-only value for a high-spin d5 configuration featuring five unpaired electrons.

The spectrum shows several intense absorption bands in the ultraviolet region (44444-33222) cm^{-1}, which are attributed to $\pi \rightarrow \pi*$ transitions, while the bands observed at higher wavelengths (32258-28901) cm^{-1} are assigned to n $\rightarrow \pi*$ transitions. The absorption band at 28089 cm^{-1} is attributed to CT. In Mn(II) complex, the d-d transitions are generally very weak and are often not clearly observed because the electronic transitions are still spin-forbidden. Even though in a tetrahedral environment, due to relaxation of the parity selection rule, they remain spin-forbidden and therefore weak. Therefore, the spectra are not detectable in the

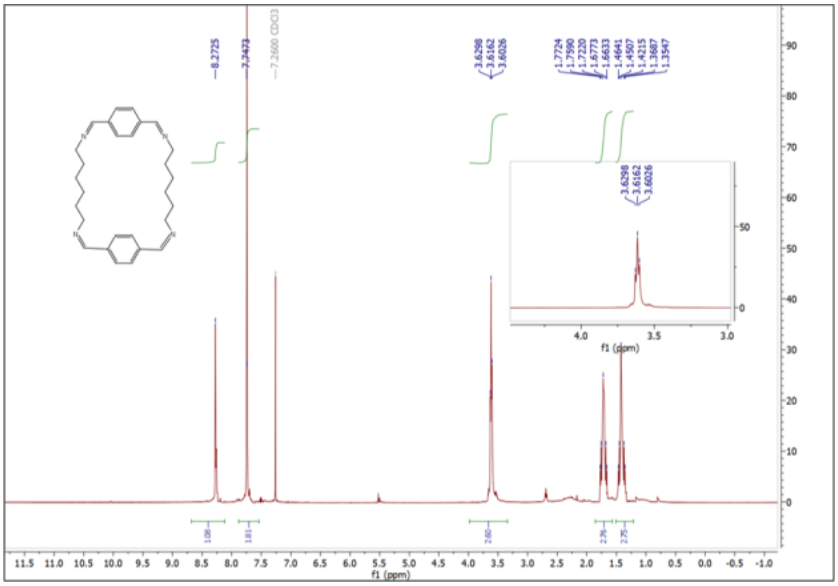

Figure 4. ^{1}H-NMR spectrum of Schiff Base Ligand.

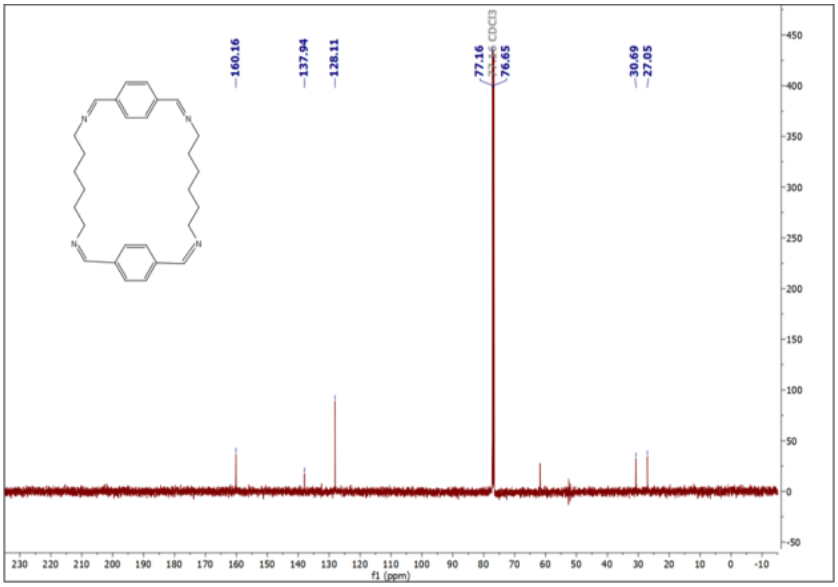

Figure 5. ^{13}C-NMR Spectrum of Schiff Base Ligand.

Table 3. Electronic transitions and magnetic moments.

symbol	Comp.	UV-visible band (cm^{-1})	Assignment	μ effect B.M	Proposed structure
L	$C_{28}H_{36}N_4$	47846, 38461 36363, 34246 29239	$\pi \longrightarrow \pi^*$ n $\longrightarrow \pi^*$	——-	——-
$[Mn_2LCl_4]$	$[Mn_2(C_{28}H_{36}N_4)Cl_4]$	44444, 36764 33222, 32258 30959, 28901 28089	$\pi \longrightarrow \pi^*$ n $\longrightarrow \pi^*$ C.T	5.7	Td
$[Fe_2LCl_4]$	$[Fe_(C_{28}H_{36}N_4)Cl_4]$	44849, 40160 38910, 34013 32573, 28571 25316, 11947	$\pi \longrightarrow \pi^*$ n $\longrightarrow \pi^*$ C.T $^5E \longrightarrow {}^5T_2$	4.6	Td
$[Co_2LCl_4]$	$[Co_2(C_{28}H_{36}N_4)Cl_4]$	43478, 38461 37037 34246 29325, 27932 16556, 14880	$\pi \longrightarrow \pi^*$ n $\longrightarrow \pi^*$ C.T $^4A_2(F) \longrightarrow {}^4T_1(P)$	3.8	Td
$[Ni_2LCl_4]$	$[Ni_2(C_{28}H_{36}N4)Cl_4]$	43859, 38910 35460, 31250 30211, 28490 21186, 13404	$\pi \longrightarrow \pi^*$ n $\longrightarrow \pi^*$ C.T $^3T_1(F) \longrightarrow {}^3T_2(F)$ $^3T_1(F) \longrightarrow {}^3A_2$	4.3	Td
$[Cu_2LCl_4]$	$[Cu_2(C_28H_{36}N_4)Cl_4]$	44247, 39525 34482, 32786 29411, 27932 23201, 19047	$\pi \longrightarrow \pi^*$ n $\longrightarrow \pi^*$ C.T $^2B_{1g} \longrightarrow {}^2A_{1g}$ $^2B_{1g} \longrightarrow {}^2E_g$	1.82	Sq
$[Zn_2LCl_4]$	$[Zn_2(C_{28}H_{36}N_4)Cl_4]$	43478, 33898 32894,31950 27700, 28652	$\pi \longrightarrow \pi^*$ n $\longrightarrow \pi^*$ C.T	Diamagnetic	Td

C.T= Charge Transfer, Td= Tetrahedral, Sq=square planer.

visible spectrum [51]. The electronic spectrum of the Fe(II) complex exhibits absorption peaks in the ultraviolet region (44849-35971)cm^{-1}, which are assigned to $\pi \rightarrow \pi*$, while those at (34013-32573) cm^{-1} correspond to n $\rightarrow \pi*$ transition. The bands in the (28571-25316) cm^{-1} may be assigned to ligand to metal charge transfer transition. In the visible region, the complex exhibits a weak broad band around 11947 cm^{-1}, corresponding to the 5E → 5T2 transition characteristic expected of a high-spin Fe(II) center d6 configuration tetrahedral geometry.

The magnetic moment value is 4.6 B.M, corresponding to four unpaired electrons [52], [53]. The UV-Vis spectrum of Co(II) complex exhibits intense absorption bands (43478-34246) cm^{-1}, which are attributed to $\pi \rightarrow \pi*$ transition, and a band at 29325 cm^{-1} is assignable to the n $\rightarrow \pi*$ transition. The absorption observed at 27932 cm^{-1} is assigned to a charge transfer transition. In the visible region, two weak, broad bands appear at 14836 cm^{-1} and 16556 cm^{-1}, arising from overlapping d-d transitions of cobalt in tetrahedral high-spin Co(II). The expected spin-allowed transition is a 4A2(F)→4T1(P) transition. The absence of 4A2(F)→ 2T2(F) and 4A2(F) → 4T1 (F) transitions is due to their low energy, which is out of the range of the instrument [54]. The magnetic moment value of 3.8 B.M for the Co(II) complex corresponds to three unpaired electrons [55].

In tetrahedral Co(II) complexes, the d-d transitions are typically broad and often overlap, resulting in fewer observable bands compared to octahedral Co(II) complexes, which usually display three well-resolved transitions. The Nickel complex spectrum shows several intense absorption bands in the ultraviolet region (43859-31250) cm^{-1}, which are assigned to $\pi \rightarrow \pi*$ and n $\rightarrow \pi*$ transitions. The band around 28490 cm^{-1} is attributed to a charge-transfer transition. In the same spectrum, two weak peaks at (21186, 13404) cm^{-1} were ascribed to the (d–d) transition 3T1(F → 3T2(F), 3T1(F)→3A2 in a tetrahedral geometry. The spin-only value for a d8 system with two unpaired electrons is 2.8 B.M, whereas tetrahedral Ni (II) complexes often exhibit higher magnetic moments due to orbital contribution.

The magnetic value of 4.3 B.M. excludes a square-planar geometry, which is usually diamagnetic for Ni(II) complexes, and supports a tetrahedral coordination environment, which is

higher than spin only due to the orbital contribution [56], [57], [58]. The electronic spectrum of the divalent Cu-complex showed bands at lower wavelength (44247-32786) $cm^{-1}$are assigned to $\pi \rightarrow \pi*$ and n $\rightarrow \pi*$ transitions. The very weak band appears at (29411-27932) cm^{-1}, which may be attributed to a ligand-to-metal charge-transfer transition. A very weak broad band appears at 23201 cm^{-1} and 19047 cm^{-1}, which is assigned to the 2B1g → 2A1g and 2B1g → 2Eg transitions [56]. The observed magnetic moment value of 1.82 B.M corresponds to one unpaired electron, as expected for a d9 configuration. Together with the electronic spectral pattern, this supports a square-planar geometry around the copper(II) ion. The Zn(II) metal complex has no discernible peak for the d10 configuration, indicating the absence of (d-d) electronic transitions. As expected for the d10 system they were found to be diamagnetic. A tetrahedral geometry has been attributed to the Zn(II) complexes based on these findings [59].

3.4 Antibacterial Activity:

The biological features of the complexes are influenced by the ligands chelating characteristics, the nature of the donor atoms, the overall charge of the complexes, the characteristics of the metal ion, the composition of the counter ions that stabilize the complex, and the geometrical configuration of the complex [60]. The C=N group, known as the azomethine group in Schiff bases, is responsible for biological activity due to its involvement in hydrogen-bond formation with the active centers of cellular constituents, thereby hindering normal cellular development. Consequently, numerous Schiff bases have been reported to exhibit antibacterial activity [61].

All synthesized compounds were evaluated for in vitro antibacterial activity against one Gram-positive bacterium (S. aureus) and two Gram-negative bacteria (E. coli and K. pneumoniae). The disc diffusion technique was used to determine the antibacterial efficacy of synthetic ligands and their corresponding coordination complex [62]. The synthesized Schiff base ligand and its metal complex were assessed for their antibacterial efficacy against bacterial strains, using Gentamicin as a positive control. The outcomes presented in Figure 7 were derived from a comparison of the biological characteristics of the ligand and its metal chelates. The common antibiotic Gentamicin was used as the standard antibacterial agent, respectively. The ligand and its complexes were dissolved in dimethylformamide (DMF) to obtain 0.001 M solutions. DMF was also evaluated under the same experimental conditions and showed no observable antibacterial activity. The results show that most complexes were more potent than the free ligand against bacteria. Furthermore, the Cu(II) complex exhibited the most potent antibacterial activity among the tested compounds, specifically against S. aureus with an inhibition zone of 13mm (lower than the Gentamicin standard) and K. pneumoniae and E. coli 8,7mm (higher than the Gentamicin standard) [61].

Other complexes also showed moderate to good activity, indicating that metal coordination is crucial for enhancing biological efficacy [49]. The Mn(II), Co(II), and Zn(II) complexes exhibit more action against S. aureus compared to Gram-negative bacteria, demonstrating inhibition zones of around 9–11 mm for S. aureus. In contrast, the free ligand (L) exhibits minimal activity against S. aureus (~6 mm), whereas DMF shows no inhibitory effect, thereby confirming that the solvent did not influence the observed antibacterial activity. This pattern substantiates the idea that metal coordination augmented the biological activity of the Schiff base ligand. Comparable Schiff base ligand-versus-complex behavior is well documented for Schiff base systems, wherein the metal complexes frequently surpass the parent ligand in diffusion-based antibacterial evaluations. The chelating ligand increases lipophilicity, thereby facilitating penetration of lipid membranes in Gram-positive bacteria.

The findings suggest that chelation enhances antibacterial efficacy [50], [63]. Lipidomic compounds are capable of traversing the fat bilayer that envelops the cell. This could be the determining factor in antibacterial action. The positive charge is more readily distributed among donor groups when ligand orbitals overlap, which reduces the polarity of metal ions in coordination. Additionally, it enhances the liposuction of complexes by increasing electron delocalization within the chelate ring.The enhanced lipophilicity of compounds enables them to penetrate lipid membranes, thereby inhibiting bacterial function [64].

3.5 DFT calculation:

3.5.1 Thermodynamic Analysis :

To obtain deeper insight into the stability and electronic behavior of the synthesized ligand and its metal complex. DFT calculations were performed at the B3LYP level using 6-311++G(d,p) for ligand atoms and LANL2DZ for the metal center at 298 K, P=1atm. The calculated thermodynamic parameters, including the zero-point energy (ZPVE), Gibbs free energy (ΔG), enthalpy (ΔH), internal energy (E), entropy (ΔS), and specific heat (Cv) of all prepared compounds are calculated to support this fundamental statement [65]. They are summarized in Tables 4 and 5 for the solvent and gas phases, respectively. The parameters provide useful information on the relative thermodynamic stability of the free Schiff base ligand and the corresponding complexes.

Table (4): In the solvent phase, all complexes show negative enthalpy values, confirming an exothermic reaction. The calculated enthalpy of the metal complexes was much lower than that of the free Schiff-base ligand. This means that the formation of the complex released heat. The formation of strong metal–ligand bonds and chelation effects cause this enthalpic stabilization. This makes the complex have a lower energy level than the uncoordinated ligand [66]. All complexes have lower Gibbs free energy than the uncoordinated ligands. Among the studied complexes, the Cu(II) complex

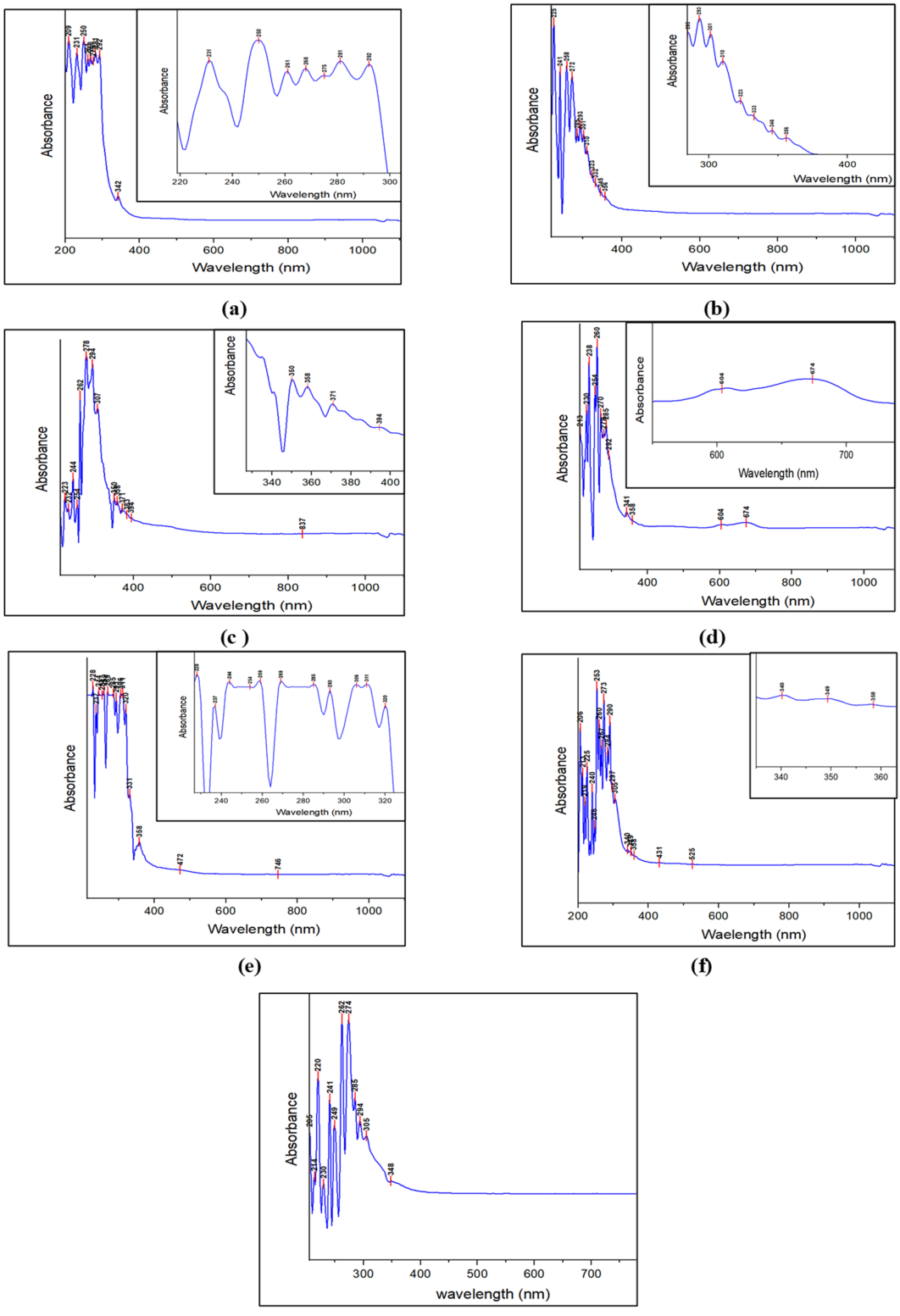

Figure 6. UV-Vis Spectra of the synthesized compounds: (a) is the Schiff Base Ligand, (b) Mn (II), (c) Fe (II), (d) Co (II), (e) Ni(II), (f) Cu(II), (g) Zn(II) Schiff Base Complexes.

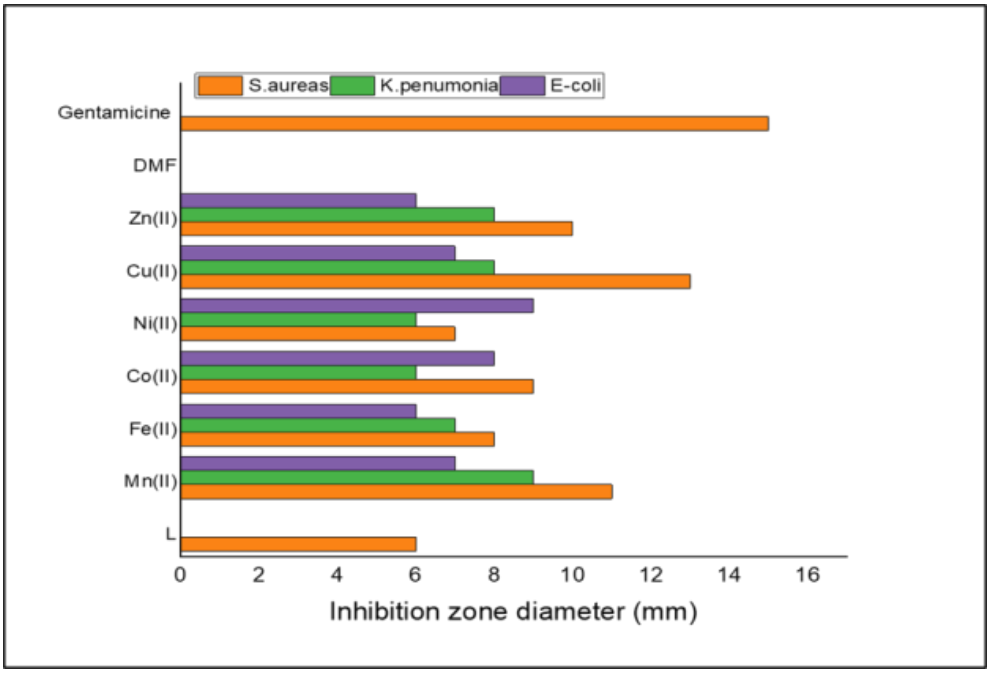

Figure 7. The antibacterial efficacy of a ligand and its metal complex in (mm).

has the highest thermodynamic stability because it exhibits the most negative Gibbs free energy. The Co(II) and Fe(II) complexes have intermediate stability with Gibbs free energy values of (1656.963 and 1613.738) a.u. respectively.

These results indicate efficient coordination between the ligand and metal centers, but with less stabilization relative to the Cu(II) complex. The Mn (II) complex is a little less stable (1574.629) a.u. than the other two. This is because it has a half-filled d^5 shape, which usually means that the ligand field stabilization energy is lower. The Ni(II) and Zn(II) complexes, on the other hand, have the least negative Gibbs free energy values (1477.454 and 1498.174) a.u. Respectively, which means they are less thermodynamically stable. This behavior is anticipated for Zn(II) since its d^{10} electronic structure does not provide ligand field stabilization. ZPVE magnitude and Cv rise post-coordination, demonstrating metal–ligand interactions add vibrational modes and molecular complexity. The complexes have more vibrational and rotational degrees of freedom than the ligand, increasing entropy. It enhances Gibbs free energy and stability [67].

3.5.2 The optimized geometry:

We employed the B3LYP/6-311++G(d,p)/LANL2DZ method and Gaussian 16 software to perform DFT calculations elucidating the influence of metal ions on the electronic characteristics of ligands. This computational approach identifies molecular structure, bond lengths, bond angles, thermodynamic parameters, and electronic characteristics, among other variables. DFT computations were employed to investigate these properties (Figure 8). The outcome reveals that modifying the central atom has a significant influence on the energy of the peripheral molecular orbitals [21].

The lengths and angles of the bonds of the prepared complexes are illustrated in Tables 6, 7, and 8. In these complexes, a Macrocyclic Structure is formed by four nitrogen-donor atoms from the chelate ligand. The measured bond lengths and angles indicate four-coordinate metal complexes with an azomethine, necessitating the participation of four electron-donating sites. These complexes have a metal-ligand proportion of 2:1 characterized by a tetradentate chelate ligand referred to as a Schiff Base Ligand.

A similar pattern is observed in the gas phase, where all complexes remain thermodynamically favored relative to the free ligand. As presented in Table 5 a comparable stability pattern is also observed in the gas phase. The Cu(II) complex remains the most stable, followed by the Co(II), Fe(II), Mn(II), Zn(II), and Ni(II) complexes. While the Gibbs free energy values calculated in the gas phase are slightly less negative than those in solution, the relative order of stability is maintained.

This finding suggests that solvation enhances the thermodynamic stabilization of the complexes, mainly through dielectric effects and weak solute–solvent interactions, but does not substantially modify their inherent stability sequence. Similar observations have been reported in published DFT investigations of Schiff-base systems, where solvent-phase calculations provide additional stabilization while preserving the preferred energetic arrangement identified in the gas phase [68].

Table 4. The thermodynamic behaviors of the ligand and its complexes in the solvent.

Comp	Zero−point Vibrational energy (a.u)	Gibbs free energy (a.u)	Enthalpy (a.u)	Internal energy (a.u)	Entropy (cal.mol^{1}K^{-1})	Specific heat, Cv (cal.mol^{1}K^{-1})
Ligand	−1308.63	−1308.69	−1308.59	403.78	205.91	122.27
$[Mn_2LCl_4]$	−1575.16	−1574.62	−1574.52	404.07	228.51	148.58
$[Fe_2LCl_4]$	−1614.27	−1613.73	−1613.63	404.74	225.81	148.11
$[Co_2LCl_4]$	−1657.49	−1656.96	-1656.85	404.11	234.72	149.20
$[Ni_2LCl_4]$	−1478.00	−1477.45	−1477.35	408.34	204.32	146.86
$[Cu_2LCl_4]$	−1759.11	−1759.18	−1759.06	403.52	246.78	150.95
$[Zn_2LCl_4]$	−1498.70	−1498.17	−1498.05	403.57	247.11	150.30

Table 5. The thermodynamic behaviors of the ligand and its complexes in the gas phase.

Comp	Zero−point Vibrational energy (a.u)	Gibbs free energy (a.u)	Enthalpy (a.u)	Internal energy (a.u)	Entropy (cal.mol^{1}K^{-1})	Specific heat, Cv (cal.mol^{1}K^{-1})
ligand	−1308.62	−1308.68	−1308.58	403.91	205.79	122.20
$[Mn_2LCl_4]$	−1574.53	−1574.59	−1574.49	403.85	230.22	148.74
$[Fe_2LCl_4]$	−1613.70	−1613.77	−1613.66	404.23	229.60	147.82
$[Co_2LCl_4]$	−1656.91	−1656.98	−1656.88	404.56	226.05	147.90
$[Ni_2LCl_4]$	−1405.43	−1405.50	−1405.39	404.52	230.53	148.06
$[Cu_2LCl_4]$	−1759.07	−1759.15	−1759.03	403.43	246.14	150.81
$[Zn_2LCl_4]$	−1498.05	−1498.13	−1498.01	403.55	249.16	150.42

atoms from the azomethine group (N3-N6) forming the corners. The bond length (M1-N3) of (2.00-2.87), (M1-N4) of (2.41-2.97),(M2-N5) of (1.97-2.24),(M2-N6) of (2.01-2.24), (M1-Cl7) of (2.24-2.44), (M1-Cl8) of (2.26-2.35), (M2-Cl9) of (2.29-2.45),(M2-Cl10) of (2.28-2.42), The measured bond lengths correspond with the bond distances documented in analogous four-coordinated systems in the literature [54],[69], [70]. A separate part of the analysis examined the calculated bond angles of the compounds. The bond angles of (N3-M1-N4), (N5-M2-N6), (Cl7-M1-N4 or Cl7-M1-N3) and (Cl10-M2-N5 or Cl10-M2-N6), are contained in the intervals [(84.9-100.62) ,(82.92-100.89), (81.458-100.62) & (82.9-165.56)] [70], [71], [72], [73].

3.5.3 Electronic properties:

Frontier molecular orbitals (FMOs) are widely recognized as the most important orbitals for describing molecular electronic structure and chemical behavior. It is widely recognized that the frontier molecular orbitals (FMOs) are the principal orbitals. In a chemical process, the two most essential orbitals are the HOMO and the LUMO, or the Highest occupied molecular orbital and the lowest unoccupied molecular orbital [74].

Subsequently, the electrical transport properties of molecules are determined by the frontier orbitals, specifically the HOMO and LUMO. The frontier orbital gap is the energy difference between the HOMO and LUMO energy levels [75], [76]. The calculated HOMO and LUMO energy values for the metal complexes, along with derived quantum chemical parameters, are presented in Table 9, as shown in Figure 9. The HOMO-LUMO energy gap of a molecule is commonly used as an indicator of various properties, including its kinetic behavior, chemical stability, optical polarizability, and chemical hardness and softness [77], [78], [79].

The electron distribution of any molecule is less variable and demonstrates minimal polarization when the HOMO–LUMO energy gap is substantial. These compounds are designated as hard molecules. When there is minimal variation in HOMO–LUMO energy, polarization is strong, electron distribution is readily manipulated, and the molecules are classified as soft molecules [80]. Assessing the HOMO–LUMO energy

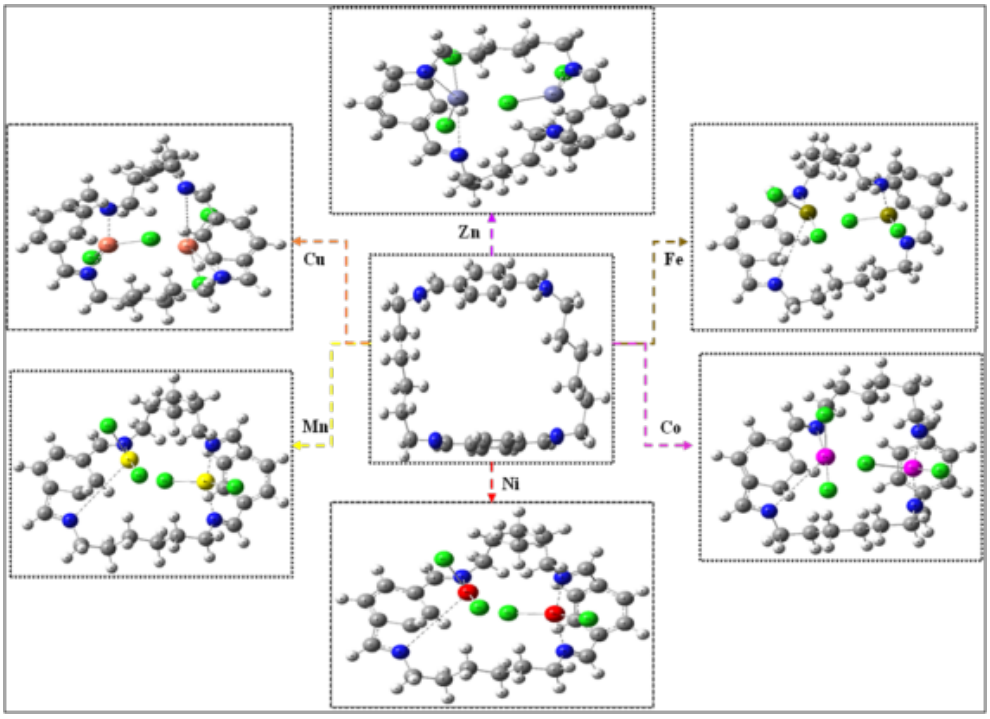

Figure 8. The optimized structure of the ligand and complexes (different colors indicate Blue -Nitrogen, White -Hydrogen, Grey- Carbon, and Green -Chlorine).

Table 6. The geometrical bond length of the synthesized compounds.

Comp	M1–N3	M1–N4	M2–N5	M2–N6	M1–Cl7	M1–Cl8	M2–Cl9	M2–Cl10
$[Mn_2LCl_4]$	2.4348	2.4955	2.1439	2.1770	2.2583	2.2620	2.4486	2.34023
$[Fe_2LCl_4]$	2.0033	2.6765	2.0605	2.1042	2.3712	2.3591	2.3236	2.39533
$[Co_2LCl_4]$	2.7759	2.4144	2.0384	2.0754	2.3004	2.3087	2.2974	2.42984
$[Ni_2LCl_4]$	2.1707	2.9768	1.9715	2.0194	2.2468	2.2503	2.2979	2.28798
$[Cu_2LCl_4]$	2.8775	2.8208	2.2087	2.2275	2.4422	2.3099	2.3537	2.42512
$[Zn_2LCl_4]$	2.6572	2.6929	2.2434	2.2496	2.3368	2.3423	2.4521	2.33937

gaps of molecules is essential for providing information. This resulted in the determination that the most stable and hardest complex was the Zn(II) complex. The calculations indicated that the molecule identified as the Cu(II) complex had the greatest softness and reactivity, with lower kinetic stability than the others. Based on the calculation The complexes can be arranged in order of increasing energy gap: Zn(II) >Fe(II) >Ni(II) >Co(II) >Mn(II) >Cu(II) [81].

This indicates that the Zn(II) complex has the largest energy gap and is therefore expected to be the hardest and least reactive species among the studied complexes. Using HOMO-LUMO energies obtained from DFT calculation at the B3LYP level employing 6-311++G(d,p) basis sets for nonmetal atoms and LANL2DZ for the metal centers, were used to calculate a variety of metrics for the complexes, including the energy gap(E) [82], [83]. Chemical hardness(η) [84], electrophilicity index(ω) [85], [86], and Electronegativity (X) [87]. The ionization potential (IP) and Nucleophiles are characterized by parameter(N) [88]. Tetracyanoethylene (TCE) is employed as a reference owing to its inherently low HOMO energy among polar organic molecules [89]. The HOMO and LUMO energies are used to calculate these quantum-chemical characteristics using formulas.

$$Electrophilicity\ Index\ (\omega): \omega = \mu^2/2\eta \quad (1)$$

$$Ionization\ energy\ (IP) = IP = -EHOMO \quad (2)$$

Table 7. Demonstrates the spatial bond angles of the synthesized compounds as determined using the B3LYP/6-311++G(d,p) method.

Comp.	N3–M1–N4	N5–M2–N6	Cl9–M2–N6	Cl9–M2–N5	Cl10–M2–N6
$[Mn_2LCl_4]$	87.092	100.809	89.620	97.612	82.912
$[Fe_2LCl_4]$	95.596	89.113	88.392	84.475	93.037
$[Co_2LCl_4]$	84.912	82.920	85.555	100.913	90.635
$[Ni_2LCl_4]$	97.476	88.969	97.742	89.149	88.03
$[Cu_2LCl_4]$	93.391	100.552	93.034	95.001	89.435
$[Zn_2LCl_4]$	100.620	87.681	88.602	90.437	99.902

Table 8. The geometric bond angles of the synthesized compounds.

Comp.	Cl7–M1–N4	CL10–M2–N5	Cl7–M1–Cl8	Cl9–M2–Cl10	Cl7–M1–N3	Cl8–M1–N4	Cl8–M1–N3
$[Mn_2LCl_4]$	156.58	158.14	154.83	158.20	87.09	99.809	102.280
$[Fe_2LCl_4]$	163.61	165.56	123.08	152.44	88.69	98.714	90.173
$[Co_2LCl_4]$	151.31	165.10	157.89	157.00	92.88	90.666	85.555
$[Ni_2LCl_4]$	160.99	162.62	155.56	162.10	82.92	88.969	90.519
$[Cu_2LCl_4]$	157.81	150.31	159.09	154.01	81.45	90.454	99.644
$[Zn_2LCl_4]$	141.80	143.84	139.61	133.12	97.68	98.602	96.824

$$Energy\ Gap\ (\Delta E_{GAP}) : \Delta E = E_{LUMO} - E_{HOMO} \quad (3)$$

Chemical Hardness (η):

$$\eta = E_{LUMO} - E_{HOMO}/2 \quad (4)$$

$$Electronegativity\ (X) = 1/2\ (E_{LUMO} + E_{HOMO}) \quad (5)$$

$$Softness\ (S) = 1/2_{\eta} \quad (6)$$

$$N = E_{HOMO}(Nu)E_{HOMO}\ (TCE) \quad (7)$$

Where TCE serves as the reference The energies of the HOMO and LUMO electron orbitals correspond to the ionization potential (IP), respectively. The Mn(II) complex has the lowest ionization potential, making it the most effective electron donor. The chemical reactivity of a molecule depends on its chemical structure. The Cu(II) complex has the highest electronegativity among the complexes, indicating the most excellent electron-withdrawing ability. The Nucleophilicity index [90]. It is essential and all the synthesized compounds (1–6) range from (3.60 to 4.90) a.u. The maximum value of N for Mn(II)complex is 4.90 a.u, the strongest Nucleophile among all [91], [92]. The electrophilicity values of all synthesized complexes are classified as the most powerful, as they all exceed 1.5 eV [93].

4. Conclusions:

This research successfully synthesized a novel macrocyclic Schiff Base Ligand via condensation. It was then coordinated with several transition-metal ions, forming well-defined metal complexes. Comprehensive spectroscopic and analytical characterizations were consistent with the proposed structures. Electronic absorption spectra and magnetic susceptibility data confirmed the expected coordination geometries around the metal centers.

The data demonstrate that the ligand forms stable binuclear complexes and acts as a tetradentate ligand. Molar conductivity investigations showed that complexes with the formula [M_2LCl_4], where M=Mn(II), Fe(II), Co(II), Ni(II), Cu(II), and Zn(II) were neutral, non-electrolytes, and all consisting of a tetrahedral geometry except Cu (II) which shows square planargeometry. Frontier molecular orbitals and optimal geometries were predicted by the DFT with the B3LYP method, using 6-311++G (d, p) and LANL2DZ basis sets for the ligand and its metal chelates, respectively. Among all the compounds, the Zn(II) complex exhibited the highest hardness and lowest reactivity, as shown by the HOMO–LUMO gap values. The antimicrobial test showed that most complexes have higher antibacterial activity than the free ligand.

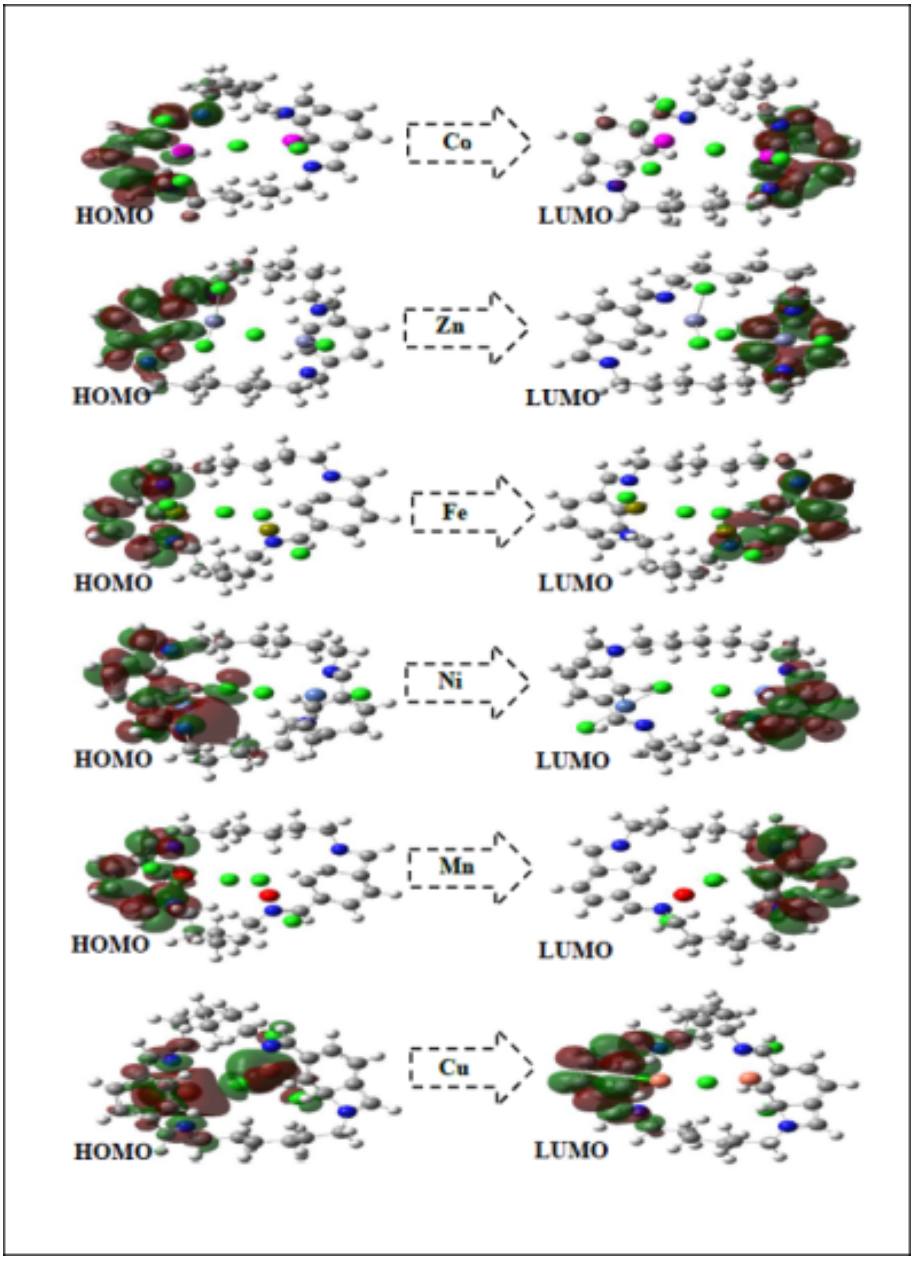

Figure 9. The HOMO and LUMO plots of the studied complexes.

Table 9. The electronic features of the prepared compounds (in a.u, one a.u. = 27.211 eV) at the level of DFT/B3LYP theory.

Comp	E_{HOMO}	E_{LUMO}	ΔE gaps	IP	η	X	S	ω	N
$[Mn_2LCl_4]$	−4.217	−3.298	0.9198	4.2178	0.4599	3.7579	1.087	15.35	4.9035
$[Fe_2LCl_4]$	−5.251	−2.685	2.5661	5.2518	1.2830	3.9688	0.389	6.137	3.86946
$[Co_2LCl_4]$	−4.615	−3.385	1.2300	4.6151	0.615	4.0001	0.8130	13.00	4.50621
$[Ni_2LCl_4]$	−5.064	−3.488	1.5756	5.0641	0.7878	4.2763	0.6346	11.60	4.05722
$[Cu_2LCl_4]$	−5.518	−4.775	0.7429	5.5185	0.3714	5.1471	1.3460	35.66	3.60279
$[Zn_2LCl_4]$	−5.309	−2.432	2.8763	5.309	1.4381	3.8709	0.3476	5.208	3.81232

5. Acknowledgements:

The authors would like to thank the Molecular Topology and Drug Design Research Unit, Department of Physical Chemistry, Pharmacy Faculty, University of Valencia, for providing access to a supercomputer with the Gaussian 16 software.

Funding: There is no financial support or sponsorship from any institute.

Data Availability Statement: The data supporting the findings of this study are available upon reasonable request from the corresponding author.

Declarations:

Conflict of interest: The authors confirm that there is no conflict of interest.

Ethical approval: This study does not involve human or animal subjects; therefore, ethical approval was not required.

Author Contributions: Marjan Marwan Islam: Conceptualization, methodology, software, validation, formal analysis, investigation, resources, data curation, and writing—original draft preparation. Salwan Idress Mohamed: review, editing, and supervision.

References

[1] Raji Sankar and TM Sharmila. Schiff bases-based metallo complexes and their crucial role in the realm of pharmacology. a review. *Results in Chemistry*, 6:101179, 2023, doi:10.1016/j.rechem.2023.101179.

[2] Sokratis T Tsantis, Demetrios I Tzimopoulos, Malgorzata Holynska, and Spyros P Perlepes. Oligonuclear actinoid complexes with schiff bases as ligands—older achievements and recent progress. *International Journal of Molecular Sciences*, 21(2):555, 2020, doi:10.30638/eemj.2008.085.

[3] Asnake Lealem Berhanu, Irshad Mohiuddin, Ashok Kumar Malik, Jatinder Singh Aulakh, Vanish Kumar, Ki-Hyun Kim, et al. A review of the applications of schiff bases as optical chemical sensors. *TrAC Trends in Analytical Chemistry*, 116:74–91, 2019, doi:https://doi.org/10.1016/j.trac.2019.04.025.

[4] Luigi Fabbrizzi. Beauty in chemistry: making artistic molecules with schiff bases. *The Journal of Organic Chemistry*, 85(19):12212–12226, 2020, doi:10.1021/acs.joc.0c01420.

[5] KJ Rajimon, Deepthi S Rajendran Nair, Dharini Srinivasaragavan, and Renjith Thomas. Integrated experimental and computational study of a fluorescent schiff base: Synthesis, characterization, electronic structure properties, and biological potentials of (1e, 1'e)-1, 1'-(1, 4-phenylene) bis (n-(2-chlorophenyl) methanimine) with a focus on molecular docking and dynamics simulation. *Chemical Physics Impact*, 8:100435, 2024, doi:10.1016/j.chphi.2023.100435.

[6] Ahmed G Ahmed, Hasan A Mohammed, Ziyad M Mustafea, and Howida A Fetouh. Facile and rapid synthesis of a new series of schiff bases: characterization and evaluation of the physicochemical properties and biological activities. *New Journal of Chemistry*, 49(31):13357–13368, 2025, doi:10.1039/d5nj02076j.

[7] Beena K Vernekar and Pradnya S Sawant. Interaction of metal ions with schiff bases having n2o2 donor sites: Perspectives on synthesis, structural features, and applications. *Results in Chemistry*, 6:101039, 2023, doi:10.1016/j.rechem.2023.101039.

[8] Subhankar Kundu, Ajoy Kumar Pramanik, Apurba Sau Mondal, and Tapan Kumar Mondal. Ni (ii) and pd (ii) complexes with new n, o donor thiophene appended schiff base ligand: Synthesis, electrochemistry, x-ray structure and dft calculation. *Journal of Molecular Structure*, 1116:1–8, 2016, doi:10.1016/j.molstruc.2016.03.01.

[9] Bhushan Nazirkar, Mustapha Mandewale, and Ramesh Yamgar. Synthesis, characterization and antibacterial activity of cu (ii) and zn (ii) complexes of 5-aminobenzofuran-2-carboxylate schiff base ligands. *Journal of Taibah University for Science*, 13(1):440–449, 2019, doi:10.1080/16583655.2019.1592316.

[10] Shalu Thakur, Ankita Jaryal, and Aman Bhalla. Recent advances in biological and medicinal profile of schiff bases and their metal complexes: An updated version (2018-2023). *Results in Chemistry*, 7:101350, 2024, doi:10.1016/j.rechem.2024.101350.

[11] Edebi N Vaikosen, Samuel J Bunu, Oyeintonbara Miediegha, Uchechi P Chilaka, Chibuzor E Echendu, and Cyril O Usifoh. Synthesis and antimicrobial evaluation of some schiff base derivatives. *Pharm. Drug Dev*, 3:1–8, 2024, doi:10.58489/2836-2322/031.

[12] Hoda Abd El-Shafy Shilkamy, Mehran Feizi-Dehnayebi, Rafat M El-Khatib, Mona MA Alharas, Rawan Al-Faze, and Ahmed M Abu-Dief. Tailored novel azomethine ligand and its cu (ii) complex for improving corrosion resistance and charge-discharge performance of ni in acidic media. *Applied Organometallic Chemistry*, 39(7):e70190, 2025, doi:10.1002/aoc.70190.

[13] Mamta and Ashu Chaudhary. Novel tetraaza macrocyclic schiff base complexes of bivalent zinc: microwave-assisted green synthesis, spectroscopic characterization, density functional theory calculations, molecular docking studies, in vitro antimicrobial and anticancer activities. *Biometals*, 37(6):1431–1456, 2024, doi:10.1002/aoc.70190.

[14] DP Singh, Ramesh Kumar, Monika Kamboj, and Kiran Jain. Synthesis, spectral, and antibacterial studies of 16-membered tetraazamacrocyclic complexes. *Journal of Coordination Chemistry*, 62(18):2995–3002, 2009, doi:10.1080/00958970903006191.

[15] Sulekh Chandra, Smriti Raizada, and Soni Rani. Structural and spectral studies of palladium (ii) and platinum (ii) complexes derived from n, n, n, n-tetradentate macrocyclic ligands. *Spectrochimica Acta Part A: Molecular and Biomolecular Spectroscopy*, 71(2):720–724, 2008, doi:10.1016/j.saa.2007.12.051.

[16] Adel AA Emara. Structural, spectral and biological studies of binuclear tetradentate metal complexes of n3o schiff base ligand synthesized from 4, 6-diacetylresorcinol and diethylenetriamine. *Spectrochimica Acta Part A: Molecular and Biomolecular Spectroscopy*, 77(1):117–125, 2010, doi:10.1016/j.saa.2010.04.036.

[17] Ahmed M Abu-Dief, Eida S Al-Farraj, Mohamed Abdel-Hameed, Nadiyah Alahmadi, Maher Fathalla, Abdullah Yahya Abdullah Alzahrani, Mashael A Alghamdi, and Aly Abdou. Design and synthesis of tunable schiff base complexes from bis-(2-oxoindolin-3-ylidene) anthracene-9, 10-dione: integrated structural, biological, and molecular modeling insights. *Computational Biology and Chemistry*, page 108682, 2025, doi:10.1016/j.compbiolchem.2025.108682.

[18] Mamta, Pinki, Subhash, and Ashu Chaudhary. Synthesis, spectroscopic characterization, density functional theory, molecular docking studies, antioxidant and antimicrobial potential of novel schiff base macrocyclic complexes of bivalent manganese. *Applied Organometallic Chemistry*, 37(6):e7095, 2023, doi:10.1002/aoc.7095.

[19] Kyle A Baseden and Jesse W Tye. Introduction to density functional theory: Calculations by hand on the helium atom. *Journal of chemical education*, 91(12):2116–2123, 2014, doi:10.1021/ed5004788.

[20] Hossein Pasha Ebrahimi, Jabbar S Hadi, Zuhair A Abdulnabi, and Zeinab Bolandnazar. Spectroscopic, thermal analysis and dft computational studies of salen-type schiff base complexes. *Spectrochimica Acta Part A: Molecular and Biomolecular Spectroscopy*, 117:485–492, 2014, doi:10.1021/ed5004788.

[21] VEYAN TAHER SULEMAN and ABDUL GHANY MOHAMMED AL-DAHER. Synthesis, characterization, density functional theory studies and antioxidant activity of novel hydrazone ligands and their metal complexes. *Oriental Journal of Chemistry*, 39(6), 2023, doi:10.13005/ojc/390624.

[22] MJEA Frisch, GW Trucks, H Bernhard Schlegel, Gustavo E Scuseria, Michael A Robb, James R Cheeseman, Giovanni Scalmani, VPGA Barone, Benedetta Mennucci, GA Petersson, et al. gaussian 09, gaussian. *Inc., Wallingford CT*, 121:150–166, 2009.

[23] Ludovid Ngouo Nogheu, Julius Numbonui Ghogomu, Desire Bikele Mama, Nyiang Kennet Nkungli, Elie Younang, and Shridhar Ramachandra Gadre. Structural, spectral (ir and uv/visible) and thermodynamic properties of some 3d transition metal (ii) chloride complexes of glyoxime and its derivatives: A dft and td-dft study. *Computational Chemistry*, 4:119, 2016, doi:10.4236/cc.2016.4401.

[24] Sultan K Alharbi, Asmaa E Hassan, Inam Omar, Bassam M Al-ahmadi, Maher Fathalla, Mona S Ragab, Mohamed R Shehata, and Ahmed M Abu-Dief. Fabrication, structural analysis, stability determination, dna interaction, and biomedical potential of some novel water-soluble schiff base complexes. *Journal of Molecular Liquids*, page 128738, 2025, doi:10.1016/j.molliq.2025.128738.

[25] Musa Alkan and Ayla Balaban Gündüzalp. Synthesis, characterization and theoretical calculations of schiff base

derived from 3-amino-1, 2, 4-triazole-5-thiol as potent antimicrobial agent. *MW Journal of Science*, 1(2):1–9, 2024, doi:10.5281/zenodo.13349694.

[26] Nighat Fahmi, Monika Upadhyay, Naveen Sharma, and Savita Belwal. Synthesis, characterization and biochemical behaviour of macrocyclic complexes of zn (ii) and co (ii) metals. *Journal of Chemical Research*, 44(5-6):336–342, 2020, doi:10.1177/1747519819893885.

[27] Sahar Shaygan, Hoda Pasdar, Naser Foroughifar, Mehran Davallo, and Fereshteh Motiee. Cobalt (ii) complexes with schiff base ligands derived from terephthalaldehyde and ortho-substituted anilines: Synthesis, characterization and antibacterial activity. *applied sciences*, 8(3):385, 2018, doi:10.3390/app8030385.

[28] Mohammad Shakir, Nausheen Bano, Mohammad Ahmar Rauf, and Mohammad Owais. Pharmacologically significant tetraaza macrocyclic metal complexes derived from isatin and 3, 4-diaminobenzophenone: Synthesis, spectral studies and comparative in vitro biological assessment. *Journal of Chemical Sciences*, 129(12):1905–1920, 2017, doi:10.1007/s12039-017-1398-8.

[29] Falih Ibadi, Emad Yousif, Ahmed Al-Ani, Mohammed Al-Mashhadani, Ali Z Al-Saffar, Ali Basem, Muna Bufaroosha, Hassan Hashim, Amani Husain, Ali H Jawad, et al. Organotin complexes with schiff's base ligands: insights into their cytotoxic effects on lung cancer cells. *Journal of Umm Al-Qura University for Applied Sciences*, 11(4):657–673, 2025, doi:10.1007/s43994-024-00170-w.

[30] Ganesan Venkatesh, Palanisamy Vennila, Savas Kaya, Samia Ben Ahmed, Paramasivam Sumathi, Vadivel Siva, Premkumar Rajendran, and Chennapan Kamal. Synthesis and spectroscopic characterization of schiff base metal complexes, biological activity, and molecular docking studies. *ACS omega*, 9(7):8123–8138, 2024, doi:10.1021/acsomega.3c08526.

[31] Nevin Turan and Memet Sekerci. Metal complexes of schiff base derived from terephthalaldehyde and 2-amino-5-ethyl-1, 3, 4-thiadiazole synthesis, spectral and thermal characterization. *Synthesis and Reactivity in Inorganic, Metal-Organic, and Nano-Metal Chemistry*, 39(10):651–657, 2009, doi:10.1080/15533170903433162.

[32] Ali Mohammad Amani, Razieh Gholizadeh, Seyed Reza Kasaee, Zahra Zareshahrabadi, Hesam Kamyab, Shreeshivadasan Chelliapan, and Sareh Mosleh-Shirazi. Biological activities of chitosan-schiff base-metal (ag and zn) nanocomposites. *Results in Chemistry*, page 102717, 2025, doi:10.1016/j.rechem.2025.102717.

[33] Sara K Yassin, JASIM MS ALSHAwI, and ZAINAb A MOHAMMEdSALIH. Novel n2o2 schiff base derived from 1, 2-hydrazinedicarboximidamide and its complexes with cu (ii), co (ii), ni (ii), mn (ii) and cr (iii): synthesis and characterization. *Oriental Journal of Chemistry*, 36(5):940, 2020, doi:10.13005/ojc/360520.

[34] Parisa Babaei, Vahideh Hadigheh Rezvan, Nastaran Sohrabi Gilani, and Somayyeh Rostamzadeh Mansour. Molecular docking and in vitro biological studies of a schiff base ligand as anticancer and antibacterial agents. *Results in Chemistry*, 7:101517, 2024, doi:10.1016/j.rechem.2024.101517.

[35] Yousif EI Hasan HA and Hussien NJ. Formation and spectroscopic studies of macrocyclic multidentate schiff-base ligand and its complexes with transition metal ions. *Diyala Journal for Pure Sciences*, 7(3):1–12, 2011.

[36] Mozaffar Asadi, Susan Torabi, and Khosro Mohammadi. Synthesis, characterization, and thermodynamics of some new unsymmetrical schiff bases of salicylaldehyde with 3, 4-diaminopyridine and their cobalt (iii) complexes. *Spectrochimica Acta Part A: Molecular and Biomolecular Spectroscopy*, 122:676–681, 2014, doi:10.1016/j.saa.2013.09.098.

[37] B Lakshmi, Prakash Gouda Avaji, KN Shivananda, Praveen Nagella, SH Manohar, and KN Mahendra. Synthesis, spectral characterization and in vitro microbiological evaluation of novel glyoxal, biacetyl and benzil bis-hydrazone macrocyclic schiff bases and their co (ii), ni (ii) and cu (ii) complexes. *Polyhedron*, 30(9):1507–1515, 2011, doi:10.1016/j.poly.2011.03.016.

[38] Abubakar Abdullahi Ahmed, Dogara Madani Joshua, and Abdulrahman Ibrahim Kubo. Synthesis and infrared spectroscopic studyof n, n-bis (4-methoxybenzylidene) thiourea with its co (ii) and ni (ii) homobinuclear complexes. *Chemical Review and Letters*, 4(3):171–177, 2021, doi:10.22034/crl.2021.291141.1112.

[39] Hadi Kargar, Mehdi Fallah-Mehrjardi, Reza Behjatmanesh-Ardakani, Mehrnaz Bahadori, Majid Moghadam, Muhammad Ashfaq, Khurram Shahzad Munawar, and Muhammad Nawaz Tahir. Synthesis, crystal structure, spectral characterization, catalytic studies and computational studies of ni (ii) and pd (ii) complexes of symmetrical tetradentate schiff base ligand. *Journal of Coordination Chemistry*, 75(7-8):972–993, 2022, doi:10.1080/00958972.2022.2092846.

[40] Ganesan Venkatesh, Palanisamy Vennila, Savas Kaya, Samia Ben Ahmed, Paramasivam Sumathi, Vadivel Siva, Premkumar Rajendran, and Chennapan Kamal. Synthesis and spectroscopic characterization of schiff base metal complexes, biological activity, and molecular docking studies. *ACS omega*, 9(7):8123–8138, 2024, doi:10.1021/acsomega.3c08526.

[41] Amina Mumtaz, Tariq Mahmud, Maryam Khalid, Huma Khan, Aatika Sadia, Malka M Samra, and Muhammad

Asim Raza Basra. Biological evaluation of synthesized schiff base-metal complexes derived from sulfisomidine. *Journal of Pharmaceutical Innovation*, 17(1):37–45, 2022, doi:10.1007/s12247-020-09476-8.

[42] Venkatesh Ganesan and Vennila Palanisamy. Synthesis, characterization, biological activity and dft calculations of schiff base ligand and metal complex. *Eurasian Journal of Science and Technology*, 5(1):56–69, 2025, doi:10.48309/ejst.2025.462773.1156.

[43] SHIKHA KATIYAR, DEVENDRA PRATAP RAO, NARENDRA KUMAR VERMA, AMIT KUMAR GAUTAM, ASHISH VERMA, CHANDRA PRAKASH SINGH, YASHVEER GAUTAM, and VIJAY SHANKAR. Dioxomolybdenum (vi) compounds of macrocyclic schiff base ligands: Preparation, characterization and antibacterial activity. *Oriental Journal of Chemistry*, 40(1), 2024, doi:10.13005/ojc/400104.

[44] Sherif O Kolade, Oluwafemi S Aina, Allen T Gordon, Eric C Hosten, Idris A Olasupo, Adeniyi S Ogunlaja, Olayinka T Asekun, and Oluwole B Familoni. Synthesis, crystal structure and in-silico evaluation of arylsulfonamide schiff bases for potential activity against colon cancer. *Crystal Structure Communications*, 80(4):129–142, 2024, doi:10.1107/S205322962400233X.

[45] Harry Chiririwa and Ochieng Aoyi. Synthesis and characterization of new tetradentate ligands. *Iranian Journal of Science and Technology, Transactions A: Science*, 41(4):1003–1009, 2017, doi:10.1007/s40995-017-0316-8.

[46] Vadim Kotlyar. Nmr chemical shifts of common laboratory solvents as trace impurities. *The Journal of organic chemistry*, 1997, doi:10.1021/jo971176v.

[47] Maryam M Alnoman, Shazia Parveen, Rua B Alnoman, Arif Khan, Mona M Khaleil, Mariusz Jaremko, Inas Al-Younis, and Abdul-Hamid Emwas. New co (ii) schiff base complexes of 3-ethoxy-4-hydroxybenzaldehyde and chlorophenyl ethylamine derivatives as potent antimicrobial agents: Design, synthesis, molecular docking, dft calculations, and in silico adme profiles. *Journal of Molecular Structure*, 1307:138021, 2024, doi:10.1016/j.molstruc.2024.138021.

[48] Esmaiel Soleimani, Sayed Ali Naghi Taheri, and Mohsen Sargolzaei. Synthesis, characterization, theoretical and biological studies of a new macrocycle schiff base whith co (ii), ni (ii), cu (ii) and zn (ii) complexes. *Journal of the Chilean Chemical Society*, 62(4):3731–3740, 2017, doi:10.4067/s0717-97072017000403731.

[49] Reddy NN Pharma D and Reddy MP. Pchhax cobalt (ii), nickel (ii), copper (ii) and zinc (ii) complexes of new n, n-bis (thiophen-2-ylmethylene) benzene-1, 2-diamine: Synthesis. *Spectroscopic and Antibacterial Studies*, 10(7):28–31, 2018.

[50] Temitayo Aiyelabola, Johan Jordaan, Daniel Otto, and Ezekiel Akinkunmi. Syntheses, characterization, antimicrobial activity and extraction studies of tetraaza macrocyclic/linear schiff bases derived from benzene-1, 4-dicarboxaldehyde and their coordination compounds. adv. *Biolog. Chem*, 11:79–105, 2021, doi:10.4236/abc.2021.113007.

[51] W AL-Kattan and E AL-Nidaa. Synthesis and characterization of mn (ii), co (ii), ni (ii) and cu (ii) complexes with schiff bases derived from terephthalaldehyde and isophthalaldehyde. *Journal of Education and Science*, 27(1):16–0, 2018, doi:10.33899/edusj.2014.161567.

[52] Mohammed Enamullah, Kazi Saima Banu, Mohammad Anwar Hossain, and Uelkue Koekcam-Demir. High-spin bis [(s or r)-n-1-(ar) ethyl-salicylaldiminato-κ2n, o]-λ/δ-iron (ii): Combined studies of syntheses, spectroscopy, diastereoselection, electrochemistry, paramagnetic, thermal, pxrd and dft/tddft. *Journal of Molecular Structure*, 1199:126947, 2020, doi:10.1016/j.molstruc.2019.126947.

[53] Assim A Sabah, Anwer M Ameen, and Abdulgany Al-Daher. Metal complexes of bis (2, 6-diamine pyridine 2, 5-hexanedione) macrocyclic schiff-base ligand: preparation, characterization and thermal study. *Iraqi Journal of Science*, pages 1885–1893, 2022, doi:10.24996/ijs.2022.63.5.3.

[54] Tsubasa Tanaka, Yukinari Sunatsuki, and Takayoshi Suzuki. Synthesis and magnetic properties of tetrahedral tetranuclear iron (ii) complexes with bis (bidentate)-type schiff bases containing imidazole groups. *Inorganica Chimica Acta*, 502:119373, 2020, doi:10.1016/j.ica.2019.119373.

[55] Ikechukwu P Ejidike and Peter A Ajibade. Synthesis, characterization, antioxidant, and antibacterial studies of some metal (ii) complexes of tetradentate schiff base ligand:(4e)-4-[(2-{(E)-[1-(2, 4-Dihydroxyphenyl) ethylidene] amino} ethyl) imino] pentan-2-one. *Bioinorganic chemistry and applications*, 2015(1):890734, 2015, doi:10.1155/2015/890734.

[56] Azza AA Abou-Hussein and Wolfgang Linert. Synthesis, spectroscopic and biological activities studies of acyclic and macrocyclic mono and binuclear metal complexes containing a hard-soft schiff base. *Spectrochimica Acta Part A: Molecular and Biomolecular Spectroscopy*, 95:596–609, 2012, doi:10.1016/j.saa.2012.04.057.

[57] Sayed M Abdallah, MA Zayed, and Gehad G Mohamed. Synthesis and spectroscopic characterization of new tetradentate schiff base and its coordination compounds

of noon donor atoms and their antibacterial and antifungal activity. *Arabian Journal of Chemistry*, 3(2):103–113, 2010, doi:10.1016/j.arabjc.2010.02.006.

[58] Sebusi Odisitse, James TP Matshwele, Ofentse Mazimba, Taye B Demissie, Morongwa Moseki, Lebogang G Julius, Mosimanegape Jongman, and Florence Nareetsile. Nickel mixed ligand complexes against drug resistant bacteria: Synthesis, characterization, antibacterial activities and molecular docking studies. *Results in Chemistry*, 6:101098, 2023, doi:10.1016/j.rechem.2023.101098.

[59] Ayman A Abdel Aziz, Ibrahim HA Badr, and Ibrahim SA El-Sayed. Synthesis, spectroscopic, photoluminescence properties and biological evaluation of novel zn (ii) and al (iii) complexes of noon tetradentate schiff bases. *Spectrochimica Acta Part A: Molecular and Biomolecular Spectroscopy*, 97:388–396, 2012, doi:10.1016/j.saa.2012.06.023.

[60] Ahmed M Abu-Dief, Rafat M El-Khatib, Salah Mohamed El Sayed, Seraj Alzahrani, Fatmah Alkhatib, Gehad El-Sarrag, and Mohamed Ismael. Tailoring, structural elucidation, dft calculation, dna interaction and pharmaceutical applications of some aryl hydrazone mn (ii), cu (ii) and fe (iii) complexes. *Journal of Molecular Structure*, 1244:131017, 2021, doi:10.1016/j.molstruc.2021.131017.

[61] Rajesh Kumar, Aditya Abha Singh, Umesh Kumar, Pallavi Jain, Atul Kumar Sharma, Chandra Kant, and Md Serajul Haque Faizi. Recent advances in synthesis of heterocyclic schiff base transition metal complexes and their antimicrobial activities especially antibacterial and antifungal. *Journal of Molecular Structure*, 1294:136346, 2023, doi:10.1016/j.molstruc.2023.136346.

[62] Gehad G Mohamed and Zeinab H Abd El-Wahab. Mixed ligand complexes of bis (phenylimine) schiff base ligands incorporating pyridinium moiety: Synthesis, characterization and antibacterial activity. *Spectrochimica Acta Part A: Molecular and Biomolecular Spectroscopy*, 61(6):1059–1068, 2005, doi:10.1016/j.saa.2004.06.021.

[63] Hoda Abd El-Shafy Shilkamy and M Rafat. Elkhatib, mona ma mehran feizi-dehnayebi. *J. Mol. Liq*, 416:126468, 2024, doi:10.1016/j.molliq.2024.126468.

[64] Zahid H Chohan, Andrea Scozzafava, and Claudiu T Supuran. Synthesis of biologically active co (ii), cu (ii), ni (ii) and zn (ii) complexes of symmetrically 1, 1-disubstituted ferrocene-derived compounds. *Synthesis and reactivity in inorganic and metal-organic chemistry*, 33(2):241–257, 2003, doi:10.1081/SIM-120017783.

[65] Priteshkumar M Thakor, Rajesh J Patel, Ranjan Kr Giri, Sunil H Chaki, Ankurkumar J Khimani, Yati H Vaidya, Parth Thakor, Anjali B Thakkar, and Jatin D Patel. Synthesis, spectral characterization, thermal investigation, computational studies, molecular docking, and in vitro biological activities of a new schiff base derived from 2-chloro benzaldehyde and 3, 3-dimethyl-[1, 1-biphenyl]-4, 4-diamine. *ACS omega*, 8(36):33069–33082, 2023, doi:10.1021/acsomega.3c05254.

[66] Abdulfattah Alkherraz, Khaled Muftah Elsherif, Awatif M Al-Arbash, Salima M Abajja, and Hana M Shawish. Conductometric investigation of schiff bases and ni (ii) ions: Stability and thermodynamics in nonaqueous solutions. *Journal of Chemistry Letters*, 6(3):157–165, 2025, doi:10.22034/JCHEMLETT.2025.501623.1278.

[67] Khaled Muftah Elsherif, Abdulfattah Mohamed Alkherraz, Hana Shawish, Salima Abajja, and Awatif Al-arbash. Thermodynamic studies of co (ii) complexation with schiff base ligands in different nonaqueous solvents. *Turkish Journal of Analytical Chemistry*, 7(2):71–78, 2025, doi:10.51435/turkjac.1606841.

[68] Almahmoud SAJ, Shek M, Alzahrani SS, Hossen S, Arfian W, and et al. Sudjarwo A. As a probe for hg 2 + in dmso solvent. *The Iraqi Geological Journal*, 594:123080, 2024, doi:10.1016/j.ica.2026.123080.

[69] Satish Chand, Monika Tyagi, Prateek Tyagi, Sulekh Chandra, and Deepansh Sharma. Synthesis, characterization, dft of novel, symmetrical, n/o-donor tetradentate schiff's base, its co (ii), ni (ii), cu (ii), zn (ii) complexes and their in-vitro human pathogenic antibacterial activity. *Egyptian Journal of Chemistry*, 62(2):291–310, 2019, doi:10.21608/EJCHEM.2018.3991.1395.

[70] Tunde Lewis Yusuf, Ibrahim Waziri, Segun D Oladipo, Mostafa S Abd El-Maksoud, Alfred J Muller, and Banele Vatsha. Copper (ii) complexes derived from halogen-substituted schiff base ligands: Synthesis, crystal structures, antibacterial activity, and molecular docking studies. *ACS omega*, 10(43):50795–50805, 2025, doi:10.1021/acsomega.4c06806.

[71] Takashiro Akitsu and Yasuaki Einaga. Syntheses, crystal structures and electronic properties of a series of copper (ii) complexes with 3, 5-halogen-substituted schiff base ligands and their solutions. *Polyhedron*, 24(18):2933–2943, 2005, doi:10.1016/j.poly.2005.06.018.

[72] Miguel Vazquez, Manuel R Bermejo, Matilde Fondo, Ana M Garcia-Deibe, Jesus Sanmartin, Rosa Pedrido, Lorenzo Sorace, and Dante Gatteschi. Monohelical complexes of a novel asymmetric n4 schiff base: Unfamiliar tetrahedral environments of manganese (ii) and iron (ii) helicates. *European Journal of Inorganic Chemistry*, 2003(6):1128–1135, 2003, doi:10.1002/ejic.200390144.

[73] Sonia A Carabineiro, Leonel C Silva, Pedro T Gomes, Laura CJ Pereira, Luis F Veiros, Sofia I Pascu, M Teresa Duarte, Sonia Namorado, and Rui T Henriques. Synthesis

and characterization of tetrahedral and square planar bis (iminopyrrolyl) complexes of cobalt (ii). *Inorganic chemistry*, 46(17):6880–6890, 2007, doi:10.1021/ic062125w.

[74] R Nalini, SM Basavarajaiah, GY Nagesh, J Mohammad, and K Ramakrishna Reddy. Synthesis, characterization, dft analysis, biological evaluation, and molecular docking of schiff base derived from isatin-isoniazid and its metal (ii) complexes. *Polycyclic Aromatic Compounds*, 43(8):7597–7614, 2023, doi:10.1080/10406638.2022.2138927.

[75] Abeer A Sharfalddin and Mostafa A Hussien. Bivalence metal complexes of antithyroid drug carbimazole; synthesis, characterization, computational simulation, and biological studies. *Journal of molecular structure*, 1228:129725, 2021, doi:10.1016/j.molstruc.2020.129725.

[76] Dalal Alhashmialameer, Gehad G Mohamed, Yasser Al-hawamy, Aly Abdou, Hassan AH Alshehri, Fatmah Alkhatib, and Ahmed M Abu-Dief. Fabrication, preparation, physicochemical characterization, and theoretical studies of some novel schiff base ciprofloxacin metal complexes: Dna interaction and biomedical applications. *Applied Organometallic Chemistry*, 38(11):e7667, 2024, doi:10.1002/aoc.7667.

[77] Hikmat A Mohamad, Karwan O Ali, Thomas A Gerber, and Eric C Hosten. Novel palladium (ii) complex derived from mixed ligands of dithizone and triphenylphosphine synthesis, characterization, crystal structure, and dft study. *Bulletin of the Chemical Society of Ethiopia*, 36(3):617–626, 2022, doi:10.4314/bcse.V36I3.11.

[78] Ahmed M Abu-Dief, Mohamed R Shehata, Asmaa E Hassan, Sultan K Alharbi, Rawan Al-Faze, Eida S Al-Farraj, and Mona S Ragab. Development of some novel hydrophilic schiff base complexes: Synthesis, spectroscopic characterization, and dft calculation dna-binding and biomedical studies supported by molecular docking approach. *Applied Organometallic Chemistry*, 39(3):e70075, 2025, doi:10.1002/aoc.70075.

[79] Saad Shaaban, Ahmed M Abu-Dief, Mohamed Alaasar, Ahmed SM Al-Janabi, Norah S Alsadun, Omar K Al Duaij, and Tarek A Yousef. Novel fe (iii), cu (ii), and zn (ii) chelates of organoselenium-based schiff base: Design, synthesis, characterization, dft, anticancer, antimicrobial, and antioxidant investigations. *Applied Organometallic Chemistry*, 39(1):e7776, 2025, doi:10.1002/aoc.7776.

[80] Aly Abdou. Synthesis, structural, molecular docking, dft, vibrational spectroscopy, homo-lumo, mep exploration, antibacterial and antifungal activity of new fe (iii), co (ii) and ni (ii) hetero-ligand complexes. *Journal of Molecular Structure*, 1262:132911, 2022, doi:10.1016/j.molstruc.2022.132911.

[81] Hanan B Howsaui, Abeer A Sharfalddin, Magda H Abdellattif, Amal S Basaleh, and Mostafa A Hussien. Synthesis, spectroscopic characterization and biological studies of mn (ii), cu (ii), ni (ii), co (ii) and zn (ii) complexes with new schiff base of 2-((pyrazine-2-ylimino) methyl) phenol. *Applied Sciences*, 11(19):9067, 2021, doi:10.3390/app11199067.

[82] Shaimaa M Elgazar, Abeer T Abd El-Karim, Walaa H Mahmoud, and Ahmed Abdou El-Sherif. Comprehensive analysis of nitrogen-oxygen schiff base derived from triazole and its metal complex: synthesis, structural characterization, and biological activities with theoretical insights for anti-helicobacter pylori, antitumor, and anti-covid-19 applications. *Egyptian Journal of Chemistry*, 68(3):169–191, 2025, doi:10.21608/EJCHEM.2024.286517.9667.

[83] RA El-Kasaby, Eida S Al-Farraj, Aly Abdou, and Ahmed M Abu-Dief. Synthesis, spectral analysis, physicochemical investigation and biomedical potential of some novel cu (ii), ru (iii) and vo (ii) complexes with anthraquinone-based schiff base supported by dft and molecular docking insights. *Journal of Molecular Structure*, 1345:143010, 2025, doi:10.1016/j.molstruc.2025.143010.

[84] Laila H Abdel-Rahman, Badriah Saad Al-Farhan, Ayman Nafady, Inam Omar, Faizah S Aljohani, Mohamed R Shehata, Ahmed M Kassem, and Ahmed M Abu-Dief. Design, preparation, physicochemical characterization, and dft calculations of some novel complexes based on bi-dentate imine ligand: Biomedical applications and molecular docking approach. *Applied Organometallic Chemistry*, 39(3):e70052, 2025, doi:10.1002/aoc.70052.

[85] Robert G Parr. Szentpaly l. v.; liu s. *Electrophilicity Index. J. Am. Chem. Soc*, 121(9):1922–1924, 1999, doi:10.1021/ja983494x.

[86] Luis R Domingo, Mar Rios-Gutierrez, and Patricia Perez. Applications of the conceptual density functional theory indices to organic chemistry reactivity. *Molecules*, 21(6):748, 2016, doi:10.3390/molecules21060748.

[87] El Hadji Mamadou Fall, Ali Zaidi, Safa Ben Amara, Mohamed Abdellahi Ami, Ndeye Arame Boye Faye, and Thorsten Koslowski. Dft investigation of the structural and spectral properties of cryptolepine: an antimalarial alkaloid. *South African Journal of Chemistry*, 78:15–23, 2024, doi:10.17159 /03794350/2024/v78a03.

[88] Sofiane Benmetir, Mohamed Chellegui, Lakhdar Benhamed, Raghad Mowafak Al-Mokhtar, Raad Nasrullah Salih, Muheb Amjad Algso, Jesus Vicente de Julian-Ortiz, and Haydar A Mohammad-Salim. Mechanistic insights into the regio-and stereoselectivity of [3+ 2] cycloaddition reactions between n-methyl-phenylnitrone and trans-

1-chloro-2-nitroethylene within the framework of molecular electron density theory. *New Journal of Chemistry*, 49(26):11191–11202, 2025, doi:10.1039/D5NJ01419K.

[89] Mar Rios-Gutierrez, Alejandro Saz Sousa, and Luis R Domingo. Electrophilicity and nucleophilicity scales at different dft computational levels. *Journal of Physical Organic Chemistry*, 36(7):e4503, 2023, doi:10.1002/poc.4503.

[90] Luis R Domingo, Eduardo Chamorro, and Patricia Perez. Understanding the reactivity of captodative ethylenes in polar cycloaddition reactions. a theoretical study. *The Journal of organic chemistry*, 73(12):4615–4624, 2008, doi:10.1021/jo800572a.

[91] Raad Nasrullah Salih, Haydar Mohammad-Salim, and Muheb Algso. Mechanistic study of n-t-butyl nitrone and cyanoacetylene [3+ 2] cycloaddition: a combined dft, docking, and admet approach. *Monatshefte für Chemie-Chemical Monthly*, 156(4):443–456, 2025, doi:10.1007/s00706-025-03300-0.

[92] Raghad Mowafak Al-Mokhtar, Haydar Mohammad-Salim, and Muheb Algso. Mechanistic study of nitrone and maleimide [3+ 2] cycloaddition: a combined dft, bet study, docking, and admet approach from the medt perspective. *Structural Chemistry*, 36(5):1707–1727, 2025, doi:10.1007/s11224-025-02455-0.

[93] Mohamed Chellegui, Raghad Mowafak Al-Mokhtar, Raad Nasrullah Salih, Lakhdar Benhamed, Sofiane Benmetir, Jesus Vicente de Julian-Ortiz, Haydar A Mohammad-Salim, and Ali Ben Ahmed. Mechanistic insights into the (3+2) cycloaddition of azomethine ylide with dimethyl acetylenedicarboxylate via bond evolution theory. *RSC advances*, 15(36):29666–29679, 2025, doi:10.1039/d5ra04992j.

تحضير وتشخيص وقياس الفعالية البيولوجية لمعقدات ثنائية السن لليكاند قواعد شيف الحلقات الكبيرة ودراسة نظرية الكثافة الوظيفية (*DFT*)

مرجان مروان اسلام * ، سلوان ادريس محمد

قسم الكيمياء، كلية العلوم، جامعة دهوك، دهوك، العراق.

* الباحث المسؤول: *marjan.islam@uod.ac*

الخلاصة

تم تحضير وتشخيص سلسلة جديدة من معقدات قواعد شيف الحلقات الكبيرة الثنائية النواة ذات الصيغة العام [M_2LCl_4] $M = Mn(II)$ ، $Fe(II)$ ، $Co(II)$ ، $Ni(II)$ ، $Cu(II)$ ، $Zn(II)$ = L 3 – (2Z,10Z,13Z,21Z) ، 10 ، 14 ، 1 – $tetraaza$ – 21 ، 12(1, ، 2 – $dibenzenacyclodocosaphane$ – (4 ، 10 ، 13 ، $tetraene$ – 21 عن طريق تفاعل تكثيفي بنسبة 2:2 بين الترفثالديهايد والهكساميثيلين ثنائي الأمين وتم الحصول علي ليكاند حلقة كبيرةمن نوع ($N4$). وتم تشخيص المعقدات المحضرة عن طريق الحساسية المغناطيسية واطياف الرنين النووي المغناطيس للبروتون 1 والكاربون 13 وطيف تحت الحمراء والاشعة فوق البنفسجية والتوصيل الكهربائي والفعالية البايولوجية ودراسة نظرية للصيغة الجزيئية والتركيب الفراغي. وتشير البيانات الطيفية والتحليلية والمغناطيسية مجتمعةً إلى وجود هندسة رباعية السطوح حول المراكز الفلزية في جميع المعقدات باستثناء معقد النحاس الثنائي $Cu(II)$ ، الذي يُظهر هندسة مستوية مربعة. كما أظهرت المعقدات سلوكًا لا غير موصل في المحلول، كما استُدل عليه من قياسات التوصيلية المولارية. استُخدمت طريقة الانتشار بالأقراص لتقييم الفعالية المضادة للبكتيريا لكلٍّ من ليكاند قاعدة شيف ومعقداته الفلزية. وقد أظهرت النتائج أن التناسق مع الفلز يعزز بصورة ملحوظة قدرة الليكاند على تثبيط نمو البكتيريا موجبة الغرام وسالبة الغرام، *Staphylococcus aureus* ، *Escherichia coli* ، *Klebsiella pneumoniae* كما أُجريت حسابات نظرية الكثافة الوظيفية (*DFT*) عند مستوى *B3LYP* باستخدام مجموعة الأساس *LANL2DZ* 6 – 331 للذرات الفلزية و $G(d,p)$++ للذرات اللافلزية. وقد وفرت هذه الحسابات الهندسيات المثلى، وطاقات *HOMO–LUMO* ، والمعلمات الثرموديناميكية، مما دعم النتائج التجريبية وقدم فهماً أعمق لتأثرات الفلزالليكاند التي تتحكم في ثباتية المعقدات وتفاعليتها.

الكلمات الدالة : ليكاند قاعدة شيف كبير الحلقة، مانح *N4* ، النشاط المضاد للبكتيريا، نظرية دالة الكثافة (*DFT*)، ثنائي النواة.

التمويل: لا يوجد.

بيان توفر البيانات: جميع البيانات المقدمة في هذه الدراسة متاحة عند الطلب.

اقرارات:

تضارب المصالح: يؤكد المؤلفون عدم وجود أي تعارض في المصالح.

الموافقة الأخلاقية: طبيعة هذه الدراسة لا تتطلب الحصول على موافقة أخلاقية.

مساهمات المؤلفين: مرجان مروان إسلام: التصور، المنهجية، البرمجيات، التحقق، التحليل الرسمي، الاستقصاء، الموارد، تنظيم البيانات، وكتابة المسودة الأصلية. سلوان إدريس محمد: المراجعة والتحرير، والإشراف.